Volume 2
Number 7
July 2023
Pages 889–1066

Energy Advances

rsc.li/energy-advances

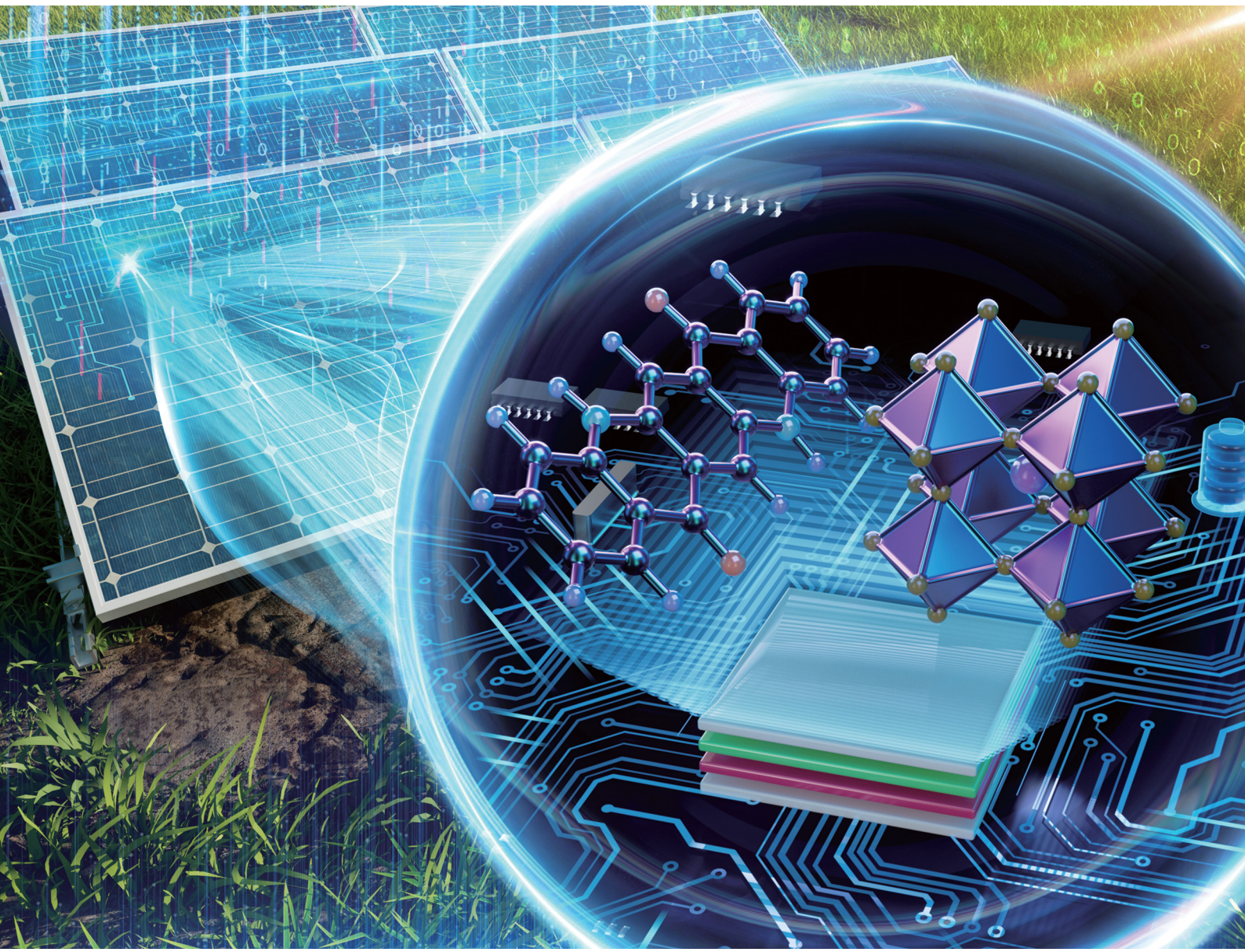

ISSN 2753-1457

ROYAL SOCIETY OF CHEMISTRY

REVIEW ARTICLE

Yuzhi Xu *et al.*

Machine learning in energy chemistry: introduction, challenges and perspectives

Energy Advances

ROYAL SOCIETY OF CHEMISTRY

REVIEW ARTICLE

View Article Online
View Journal | View Issue

Check for updates

Cite this: *Energy Adv.*, 2023, 2, 896

Machine learning in energy chemistry: introduction, challenges and perspectives

Yuzhi Xu,†[ad] Jiankai Ge †*[b] and Cheng-Wei Ju *[c]

With the development of industrialization, energy has been a critical topic for scientists and engineers over centuries. However, due to the complexity of energy chemistry in various areas, such as materials design and fabrication of devices, it is hard to obtain rules beyond empirical ones. To address this issue, machine learning has been introduced to refine the experimental and simulation data and to form more quantitative relationships. In this review, we introduce several typical scenarios of applying machine learning to energy chemistry, including organic photovoltaics (OPVs), perovskites, catalytic reactions and batteries. In each section, we discuss the most recent and state-of-art progress in descriptors and algorithms, and how these tools assist and benefit the design of materials and devices. Additionally, we provide a perspective on the future direction of research in this field, highlighting the potential of machine learning to accelerate the development of sustainable energy sources. Overall, this review article aims to provide an understanding of the current state of machine learning in energy chemistry and its potential to contribute to the development of clean and sustainable energy sources.

Received 2nd February 2023,
Accepted 24th April 2023

DOI: 10.1039/d3ya00057e

rsc.li/energy-advances

Open Access Article. Published on 24 April 2023. Downloaded on 2/11/2026 2:23:30 PM.
This article is licensed under a Creative Commons Attribution-NonCommercial 3.0 Unported Licence.

1. Introduction

Energy consumption is rising accompanied by population growth and industrialization.[1] Currently, fossil fuels such as coal, oil, and natural gas still dominate the global energy consumption.[2,3] However, the burning of fossil fuels leads to a huge emission of carbon dioxide, which contributes to global warming and has negative impacts on the environment and human health.[4,5] Therefore, it is increasingly important to develop sustainable and clean sources of energy in order to replace fossil fuels. Many attempts have been made over the last few decades to accomplish energy conversion and storage with high efficiency and little pollution, such as solar, wind, water, biofuel, and hydrogen.[6] To be more specific, in the last 10 years, there has been significant progress in the field of sustainable and clean energy (Fig. 1). It is also an area that will

[a] *Department of Chemistry, New York University, New York, New York 10003, USA*
[b] *Chemical and Biomolecular Engineering, University of Illinois at Urbana-Champaign, Urbana, Illinois 61801, USA. E-mail: jiankai2@illinois.edu*
[c] *Pritzker School of Molecular Engineering, The University of Chicago, Chicago, Illinois 60637, USA. E-mail: cwju@uchicago.edu*
[d] *NYU-ECNU Center for Computational Chemistry at NYU Shanghai, Shanghai 200062, China*
† These authors contributed equally to this work.

Yuzhi Xu

Yuzhi Xu is currently a graduate research fellow at the NYU-ECNU Computational Chemistry Center at NYU Shanghai and pursuing his PhD degree at the Department of Chemistry at New York University (NYU). He received his bachelor degree from the College of Materials Science and Engineering, South China University of Technology in 2021. His research interest is in the development of novel computational methods and artificial intelligence applications in chemistry.

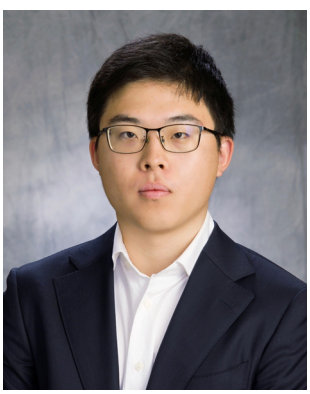

Jiankai Ge

Jiankai Ge is a graduate student of the University of Illinois, Urbana-Champaign, Department of Chemical and Biomolecular Engineering. He obtained his BS degree in chemistry from the University of Science and Technology of China, in 2021. Currently, he is working on computational design and multiscale modeling tools for polymer upcycling research.

© 2023 The Author(s). Published by the Royal Society of Chemistry

Open Access Article. Published on 24 April 2023. Downloaded on 2/11/2026 2:23:30 PM.
This article is licensed under a Creative Commons Attribution-NonCommercial 3.0 Unported Licence.

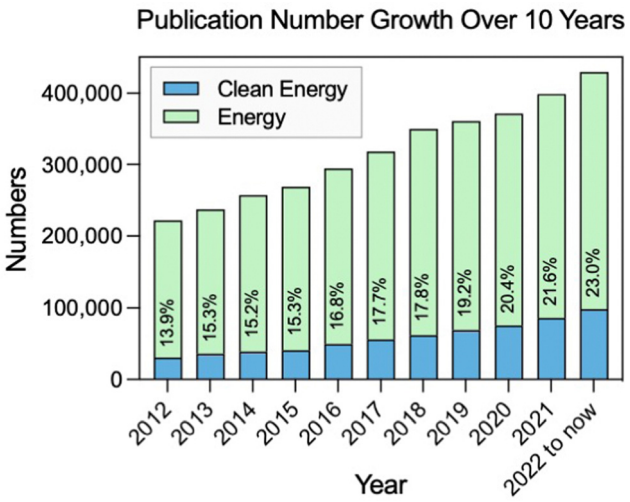

Fig. 1 Change in the number and percentage of publications with clean energy and containing energy topics in the last decade (source: Web of Science).

continue to be a focus of research and development in the forthcoming years.[7–9]

Photovoltaics (PV) is one of the clean energy technologies that utilize solar energy and has gained more and more attention. More particularly, solar energy is a source of energy that can be considered as physically infinite. Therefore, adopting solar energy is regarded as the most promising solution to address the energy crisis.[10] PV can be divided into three categories: silicon-based solar cells, organic solar cells (OSCs), and the increasingly popular perovskite solar cells (PSCs).

Currently, over 90 percent of the global PV market is dominated by crystalline silicon solar cells.[11] Silicon-based solar cells are mature and commercially available for large-scale manufacturing. However, in most buildings and agricultural production sites, the opaqueness and weight of crystalline silicon prevent it from being used as a cover.[12] OSCs and PSCs are considered as potential alternatives to silicon-based solar cells, as they have the potential to be light weight, flexible, and produced at a lower cost. Nevertheless, compared to silicon-based solar cells, OSCs and PSCs are still in the development stage.[13] The high power conversion efficiency (PCE), long-term stability and less efficiency loss while scaling up are the main challenges for OSCs and PSCs.[14]

Computational design of materials has become an essential part of PV design.[15–17] By using computational methods, researchers can simulate and predict the performance of different materials and devices without costly and time-consuming experimental trials. Such methodology can greatly accelerate the materials design and device optimization process. In the past few decades, computational chemistry methods have mainly employed first principles method.[18,19] One of the main advantages of first principles methods is that they can accurately and non-empirically predict the electronic and optical properties of materials, including the energy levels of electrons and holes, band gaps, and the absorption spectrum. In recent years, machine learning, a statistics-based technology, has become an important part of computation-aided materials design.[20,21] Through machine learning, researchers can not only bypass complex formulas to explore relationships between different values but also generate novel compounds and materials. Many parameters in materials or devices for PV cannot be simply derived from theoretical equations or calculated using the first-principles method, while the usage of machine learning greatly facilitates research in these areas.

In addition to PV, the catalytic reaction is also an efficient tool in sustainable and energy chemistry. A lot of catalysts have been developed to accelerate different types of chemical reactions, like the oxygen reduction/evolution reaction (ORR/OER), hydrogen evolution reaction (HER), CO_2 reduction reaction (CO_2 RR), *etc.*[22–24] However, the catalytic ability is limited by multiple factors such as synthesis conditions, morphology, measurement methods, *etc.*[25–27] It is hard to develop theories or models to describe catalytic systems. Machine learning, with the benefits of multi-factor fitting and identifying trends, has great potential in catalytic fields. Similarly, with the help of machine learning, researchers may be able to improve the understanding of the structure–function relationship and predict the catalytic ability, thereby guiding the synthesis of catalysts.

To date, there are already many websites, books, and reviews on machine learning in chemistry or energy that describe machine learning algorithms and the related research process.[28–30] To gain a better understanding of basic machine learning concepts such as what an algorithm is, what a dataset is, and how to manipulate and use machine learning, refering to these excellent works may help in comprehending the machine learning process.[31–33] This review provides a perspective on input types, task types and state-of-the-art (SOTA) performances when using machine learning in energy chemistry. We expect that this review could help chemists and materials scientists to gain more insight into how machine learning empower the development of energy chemistry.

Here, we will introduce how machine learning could optimize and accelerate the development of energy chemistry, especially in designing of materials. More specifically, this review focuses on the recent advancements, applications, and future prospects of machine learning in the fields of PV, catalysis and batteries. These are essential areas of energy chemistry, where machine learning techniques have been applied to improve the prediction, design, and optimization of material properties. In Section 2, we provide a brief introduction to organic photovoltaics (OPV) and delve into the structural and electronic descriptors. We further discuss the development of *de novo* design of OPV materials. In Section 3, we summarize multiple types of features and prediction tasks for perovskites. After that, we discuss how machine learning helps in perovskite discovery through experiments and auto-synthesis. In Section 4, developing atomistic potentials and the prediction for heterogeneous catalytic reactions are presented. As a practical application, battery design and management are reviewed with typical examples in Section 5. Finally, a perspective on developing novel machine learning-based methodologies aimed at solving chemistry problems and their applications in energy chemistry is proposed. With the assistance

Open Access Article. Published on 24 April 2023. Downloaded on 2/11/2026 2:23:30 PM.
This article is licensed under a Creative Commons Attribution-NonCommercial 3.0 Unported Licence.

of machine learning, scientists can benefit from developing materials designs on different scales, from predicting and optimizing properties, fitting atomistic force fields, to managing systems.

2. Organic photovoltaics

Compared with traditional crystalline silicon PVs, OPVs have the advantages of light weight, low-cost, and flexibility.[34,35] One of the major advantages of commercial OPVs is that they can be solution-processed, which means that they can be cost-effectively produced on large-area PVs.[36] OPVs have been under development for several decades, but their performance still lags behind that of crystalline silicon PVs, particularly in terms of PCE. It is imperative to search for novel and efficient OPV materials. Many factors can affect OPVs, such as electronic structure properties (HOMO, LUMO, and bandgaps), interfaces, and bulk heterojunction (BHJ) mixing. With the advent of machine learning, it is now possible to quickly predict these physical properties or efficiency before experiments, thereby saving time, resources, and manpower. Therefore, machine learning can be used as a powerful tool for high-throughput screening in the development of OPVs.[37] Many accessible material databases that have been created based on previous calculation works provide a good data environment for using machine learning in exploring promising OPVs.[38–40] Besides, researchers used to manually collect a large amount of data from previous papers to establish training databases.[41,42] Leveraging these databases, many precise OPV prediction models have been proposed.

2.1 OPV descriptors

Descriptors build a bridge between computer algorithms and physical understanding, which is critical for effectively predicting new materials or properties. Due to the complexity of OPV structures, the understanding of the quantitative structure–property relationship (QSPR) for OPVs is still inadequate even now. Thus, researchers invest significant effort in developing descriptors to uncover more hidden information within the structure of OPVs.

There are multiple types of descriptors used in the process of converting raw data into features for OPVs, and these types can be divided into two categories: physical property representation and chemical structure representation. In physical property representation, researchers usually directly use electronic structure parameters or measurement values as the features. When constructing features using physical property data from different papers, it is important to ensure similar measurement conditions to avoid model bias or deviation. In chemical structure representation, various methods based on different structure description dimensions can be employed to describe the structure. It is important to note that these methods are often accompanied by a loss of information when converting a chemical structure to a feature. Therefore, the method of converting chemical structures into features may vary depending on the specific situation.

It is important to choose the suitable number and types of descriptors as features because adding more features in the model does not guarantee better prediction results. The inappropriate descriptors can add redundant information to the model and too much features may lead to model overfitting. Besides, it may also increase the dimensionality of the data, making the model training more expensive and difficult. Hence, feature engineering is usually required after manually selecting the descriptors to optimize the performance of the model.[43] In actual practice, chemical structure descriptions and electronic descriptions typically complement one another.[44]

2.1.1 Chemical structure representation. In machine learning in chemistry, the most commonly used descriptors are chemical structure descriptors. Compared to values or parameters based on manual measurements, molecular structures are a precise input for machine learning algorithms requiring accurate data for training because chemical structures are not influenced by experiments. Chemical structural descriptors have some benefits: (1) chemical structural descriptor inputs are suitable for all molecule-based models, regardless of their downstream task. This universal input even contributes more than experimental values in the model. Zhao *et al.* investigated the impact of several descriptors on the prediction of PCE and discovered that structural descriptors have the most contribution to machine learning models.[45] (2) Accuracy of chemical structural descriptors is not affected by noise, occasional experimental errors or hidden parameters.[46] Therefore, a combination of different structural databases is possible. (3) Chemical structure representations are flexible and adaptable. Researchers can use language modification methods to boost the precision of chemical structure representations. Generally, molecular structures can be represented by simplified molecular-input line entry system (SMILES) character strings.[47] This simple representation is widely used in chemical structure databases, chemical drawing software, molecular modeling and recognized as the standard compound representation for chemical information processing tasks. It is easy to expand SMILES to novel representation by adding topological or atom environmental to capture precise molecular information from the structure.[48] To adapt the deep learning, O'Boyle *et al.* and Krenn *et al.* proposed DeepSMILES and self-referencing embedded strings (SELFIES) for molecule generation, respectively (Fig. 2a).[49,50] Besides character representation, the chemical structure can be represented as a compact numerical representation based on the presence of pre-defined substructures (Fig. 2b). This method is named molecular fingerprints. In polymers, the chemical fragment representations could improve the model performance. In our previous work, we developed the multidimensional fragmentation descriptors method to boost the prediction accuracy of linear conjugated polymers (Fig. 2c).[51] In addition to the abovementioned descriptors, complex atom-based structure representations combine the electronic structure information and topological structure information to provide a more comprehensive understanding of a compound's structure.[52,53]

In the chemical structure representation of OPVs, the whole polymer cannot be described directly using the machine learning algorithm for its complex components. As an approximation method, researchers usually adopt individual monomers to

© 2023 The Author(s). Published by the Royal Society of Chemistry

Open Access Article. Published on 24 April 2023. Downloaded on 2/11/2026 2:23:30 PM.
This article is licensed under a Creative Commons Attribution-NonCommercial 3.0 Unported Licence.

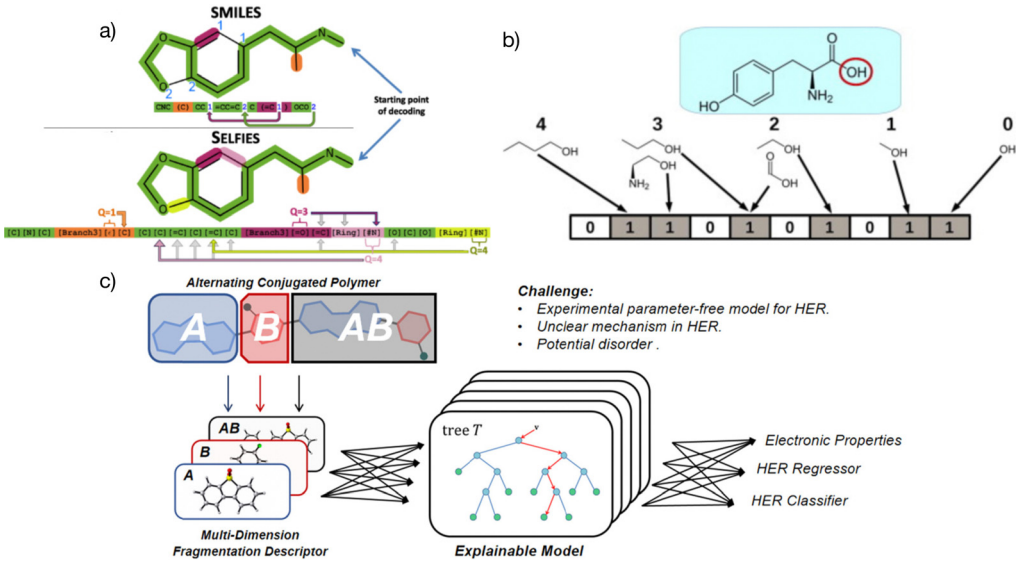

Fig. 2 (a) Specific representation coding and differences between SELFIES and SMILES, with SELFIES having a more complex structure than SMILES.[50] Reproduced from ref. 50 under the terms of the Creative Commons Attribution 4.0 license from IOP Publishing. (b) Simple representation of molecular fingerprints.[54] Reprinted (adapted) with permission from ref. 54. Copyright 2014 Elsevier. (c) The multidimensional fragmentation descriptors strategy in a linear alternative polymer; A and B represent different fragments in the polymer and A–B stands for a monomer in the polymer. The features from different input dimensions work together and boost the prediction accuracy of the linear alternative polymers.[51] Reprinted (adapted) with permission from ref. 51. Copyright 2021 American Chemical Society.

represent the polymers. Therefore, the process of describing small molecule and polymer structures is similar. In many cases of small molecule or protein design, 3D coordinates or 4D descriptors are useful as they provide detailed information about the molecular structure and conformation.[55] However, the OPV structures are often more complex, and the use of these high dimensional descriptors may not be as effective. Besides, researchers are more concerned with OPV functionality than with subtle changes in the absolute position. Thus, 3D or 4D descriptors are rarely employed in the OPV machine learning work. In actual practice, structural descriptors are mainly classified into 2D and 3D categories. 2D descriptors can be mainly divided into SMILES (including different kinds of SMILES, such as canonical SMILES and SMILES with atomic mapping), InChI, Tensors and others. 3D descriptors can be divided into voxels, Coulomb matrix, tensor field networks and potential energy surface method. Using the concept of physical descriptors, Elton *et al.* introduced general descriptor production rules in two and three dimensions.[56] Recently, the majority of OPV machine learning studies have used molecular fingerprints as the primary structure representation. This is because molecular fingerprints not only contain the original structure of the molecule but also capture some information from the surrounding atomic environment at a 2D level. This type of environmental information is generally in the range of 4–6 atoms such as extended-connectivity fingerprints (ECFP4 and ECFP6).[57] Although molecular fingerprints lose long-range structural information, it is believed that with a large enough dataset, the environmental information supplemented by subsegments can still capture this information. This is because OPV molecules have relatively fixed building blocks of the backbone structure. Note that very few OPV works simply use structures as the only descriptor. Generally, multiple descriptors including PV parameters and chemical structure information are featured together.

In many cases using fingerprints as descriptors, random forest (RF) and boosting decision tree (BDT) are the most suitable models in OPVs.[58,59] Sun *et al.* manually constructed a database of more than 1700 experimentally tested real donor materials including both polymers and small molecules (with a median PCE of 3.48%).[60] They compared the performance of image representation, ASCII strings, and seven molecular fingerprints in the binary classification of "high" or "low" PCE (two thresholds are 3.00% and 10.00%) with the algorithms of the back propagation neural network (BPNN), deep neural network (DNN), RF and support vector machines (SVMs). Besides, they also researched the influence of different lengths of the fingerprints. They found that using RF with daylight fingerprints[61] an average prediction accuracy of 86.67% could be achieved and explored whether the fingerprints whose length is longer than 1000 bits including sufficient chemistry information are suitable candidates for building descriptors in PCE prediction models. Furthermore, Wu *et al.* established a small database of 565 donor/acceptors (D/A) combinations and used a fragment fingerprint method to build a PCE prediction model.[62] In their work, the authors employed five different model methods including linear regression (LR), boosted regression trees (BRT), multinomial logistic regression (MLR), RF and artificial neural network (ANN) to perform ternary classification of PCE (power conversion efficiency) using thresholds of 7% and 11%. Among these methods, RF achieved the highest performance with 65.2% accuracy in the ternary classification of high-level PCE (>11%). They discovered six novel D/A combinations

Open Access Article. Published on 24 April 2023. Downloaded on 2/11/2026 2:23:30 PM. This article is licensed under a Creative Commons Attribution-NonCommercial 3.0 Unported Licence.

after virtual screening. After that, they compared the PCE values of the new materials with model prediction values and found that RF prediction values are closest to experimental values.

As mentioned before, small molecules are treated as monomers using fingerprints in OPVs without considering the molecular weight and binding situation. In some cases, if the structure is complex, it can lead to large deviations in material predictions. Nagasawa *et al.* used MACCS fingerprints and bandgaps, the HOMO, and weight-averaged molecular weight as the input with ANN and RF methods to build a PCE prediction model (Fig. 3).[63] However, the predicted PCE of selected OPV molecules in the Harvard Clean Energy Project dataset was about 5.0%–5.8% while the experimental device values were 0.47 ± 0.04%. They concluded that the deviations between the machine learning and experiment values are due to the direction of combining and low molecular weight. Additionally, as an extension of the molecular structure, molecular graphs converted from SMILES can also be the structural descriptors in building PCE machine learning models. Eibeck *et al.* used the graph neural network (GNN) model and attention fingerprint model found by Xiong *et al.*[64] in the PCE prediction and reported achieving the Pearson correlation coefficients of 0.68 and 0.57.[65] In the field such as retrosynthesis[66] and chemical reaction prediction,[67] the molecular graph performed well, and with the development of the GNN and machine learning in chemistry, this method will contribute more to OPVs.

2.1.2 Electronic descriptors. In OPVs, there are many physical parameters achieved through experiments or simulations. A few descriptors are from the raw experimental data values, mainly focusing on the short-circuit current (J_{SC}), open-circuit voltage (V_{OC}), fill factor (FF), and PCE. Usually, the measured parameters are used as targets to be predicted rather than features. This is because the experiment-free machine learning model can be used in the virtual screening of new materials. Also, many electronic descriptors are from properties (*e.g.*, HOMO and LUMO, bandgap, reorganization energy (λ), dipole moment (μ), *etc.*) which are usually achieved through calculation. In previous research, more detailed discussions about electronic descriptors were documented.[53,68] Besides, new electronic descriptors can be derived from linear combinations of defined electronic descriptors. Sahu *et al.* defined two new descriptors, LUMO and HOMO differentials from the donor and acceptor, and verified the poor correlation between these attributes. This result suggests that they can be treated as independent descriptors (Fig. 4).[53]

Combining electronic descriptors with visualizing decision tree models, researchers can gain physical insights and experimental guidance from the trained models.[51,70] To visualize a decision tree, the model is represented graphically as a tree-like structure. In the tree-like structure, there are four main types of nodes: root nodes, leaf nodes, internal nodes, and branch nodes. To be more specific, input data are located at the root nodes and the predictions are at the leave nodes. Each branch of the tree

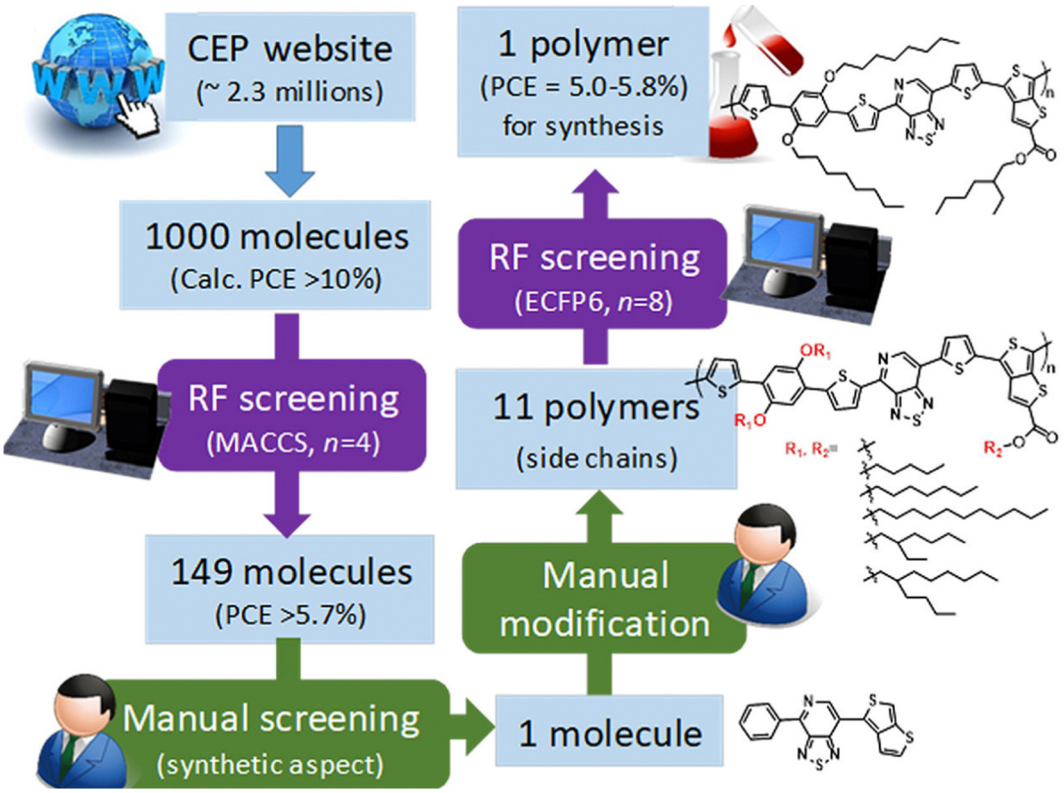

Fig. 3 Workflow of the high PCE OPV material selection by Nagasawa *et al.*[63] Reprinted (adapted) with permission from ref. 63. Copyright 2018 American Chemical Society.

© 2023 The Author(s). Published by the Royal Society of Chemistry

Open Access Article. Published on 24 April 2023. Downloaded on 2/11/2026 2:23:30 PM.
This article is licensed under a Creative Commons Attribution-NonCommercial 3.0 Unported Licence.

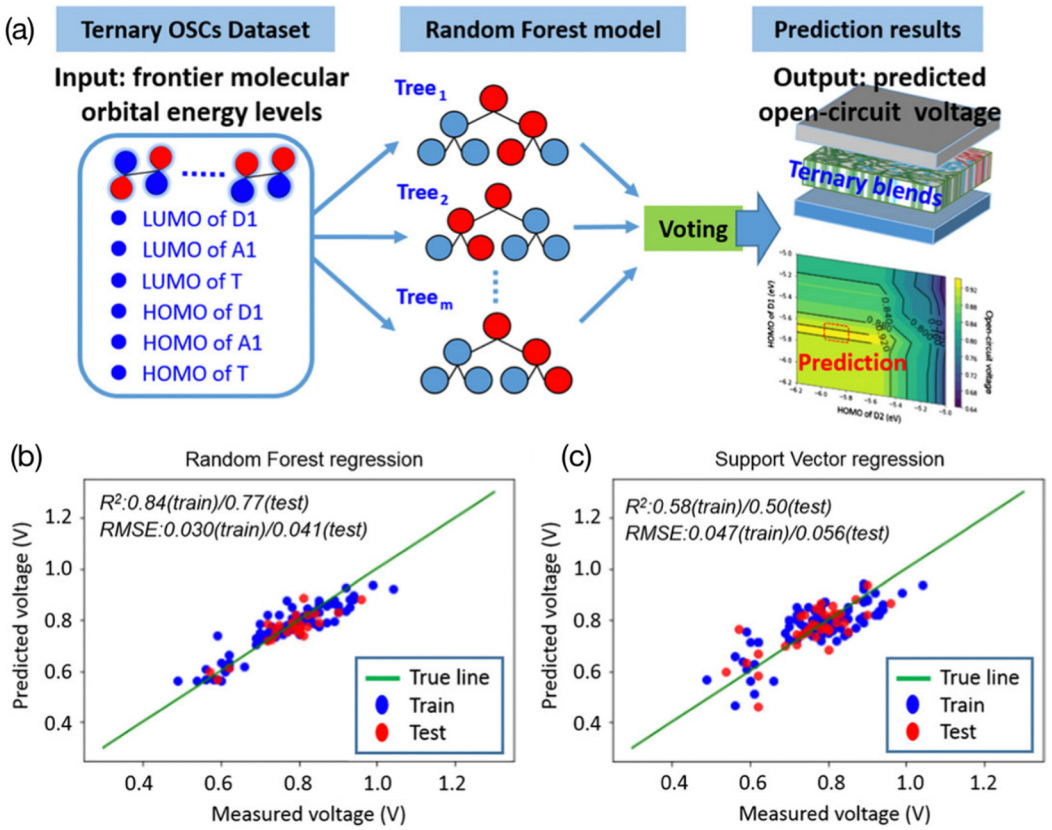

Fig. 4 (a) Using the values of the HOMO and LUMO as features in the ternary OPV V_{OC} prediction model. (b) The RF model and (c) SVM model.[69] Reproduced from ref. 69 under the terms of the Creative Commons Attribution License from Wiley.

represents a decision made on the attributes, and the internal node shows the test on the attributes. This tree is constructed by repeatedly splitting the data based on the attributes that provide the most information gain. This process will continue until the stopping criteria are met. Decision tree visualization can help to understand the structure and decisions made using the model and can provide direct insights into the relationships between the input variables and the output predictions. For example, Lee used a ternary OPV machine learning model to verify the correlation between the electronic properties (HOMO and LUMO from donors, acceptors, and third components, respectively) of various materials and their PCE[69] (Fig. 5). He employed the feature ranking mechanism of the RF algorithm to rank the contribution of each feature to the V_{OC} and concluded that the donor's LUMO and HOMO had a primary impact on the V_{OC}. Furthermore, he established an RF model for binary classification, with a threshold of 9%. After analyzing the logical flowchart of the classification of the two groups, it was found that the LUMO and HOMO of the donor, as well as the HOMO of the acceptor, were the key values that contributed to the classification model. This result is consistent with previous work in the field, which also identified these features as important for the classification of the two groups.

2.2 *De novo* materials design

In OPVs, the main goal of using machine learning is to explore new materials. No matter whether chemical structural descriptors or electronic descriptors are used, the applications in which they are used are mostly focused on supervised learning, which requires the manual definition of data labels. However, the supervised learning model can only use the fragmentation methods to generate novel OPV molecules. In this method, researchers adopt a trained supervised learning model to score the manually defined fragments or building blocks from defined fragment combination libraries. Such libraries could be established using either expert knowledge or traversal searching methods.[72,73] After identifying the well-performing fragments, researchers usually combine them into novel compounds. A trained prediction model is used to predict the properties of candidates.[74] After that, the candidates with the desired properties are selected for further study and experimentation. A typical benefit of this approach is that new compounds are more likely to be synthesizable under real-world conditions. However, based on this method, chemical space is limited by the way of combinations and the types of fragments, which limits the diversity of new molecules. Recently, there has been an increasing number of researchers showing interest in the *de novo* design of compounds using deep learning methods.[75–77] Using *de novo* design methods, researchers can generate new molecules without any pre-defined building blocks.

Nigam *et al.* proposed a molecular generative neural network model based on the SELFIES description method for inverse molecular design, named superfast traversal, optimization, novelty, exploration and discovery (STONED) and the workflow

Open Access Article. Published on 24 April 2023. Downloaded on 2/11/2026 2:23:30 PM.
This article is licensed under a Creative Commons Attribution-NonCommercial 3.0 Unported Licence.

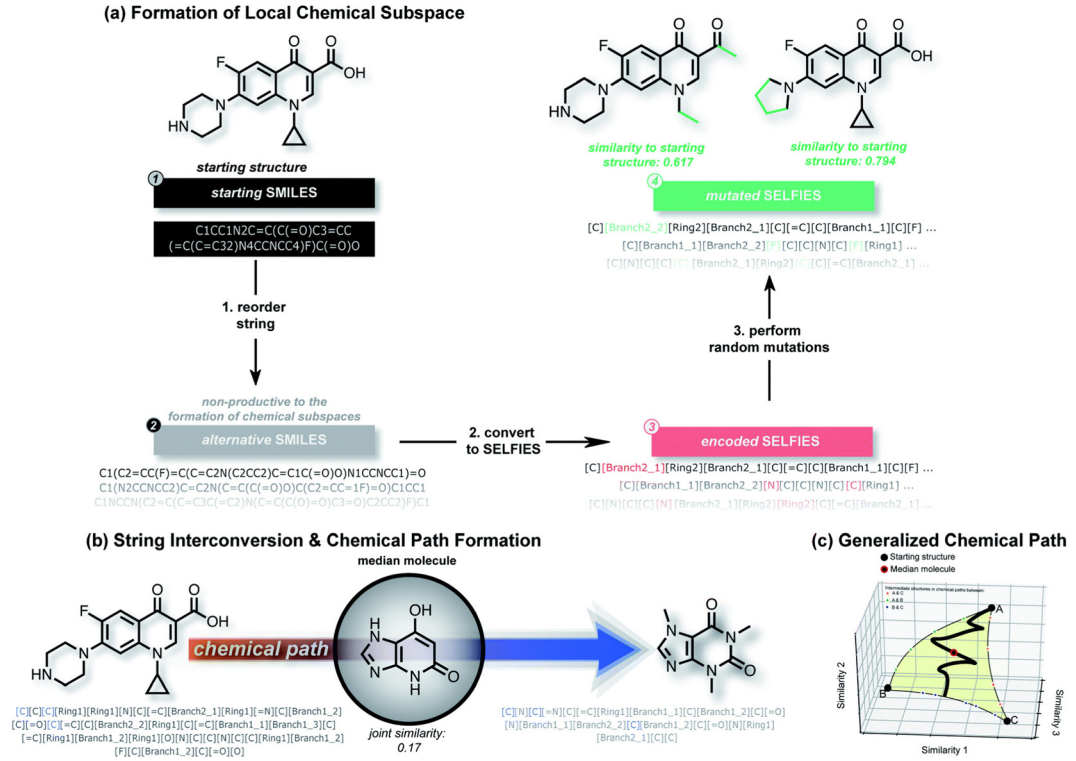

Fig. 5 An overview of the STONED. (a) shows how STONED obtains the chemical subspaces. Reordering the SMILES string within the same molecule can generate different orders of SELFIES. Random mutation in SELFIES can yield vast different molecules with similar structures. (b) and (c) demonstrate how to form the path generated by two reference molecules and how to find the median molecule along the path, respectively.[71] Reproduced from ref. 71 with permission from the Royal Society of Chemistry.

is shown in Fig. 5. This model enables structure enumeration in chemical space and the discovery of transformation trajectories between any two molecules.[71] The researchers utilized the ability of SELFIES to generate multiple structures by adding, deleting and changing random characters while maintaining a rational chemical structure. This allowed them to form local chemical subspaces. They also defined the chemical space path as a finite step change between two molecules to achieve a transformation from one end to the other. They tried to find the median molecule, which is similar to several reference molecules, in the path of the two reference molecules. In the application of the discovery of new OPV molecules, they took three properties (high LUMO energy, high dipole moment and high HOMO–LUMO energy gap) as end molecules and tried to find median molecules among them.

For the *de novo* design of a molecule, it is important to select the benchmarking task for the design. Currently, most of the insight into which threshold in machine learning to use derives from the researcher's own judgment and experience. A public benchmark is helpful in comparing the performance of different models. Nigam *et al.* reported a series of benchmarks named TARTARUS for designing molecules including OPV molecules.[78] They demonstrated the utility of the TARTARUS benchmarks by evaluating several mature algorithms such as VAEs, long short-term memory hill climbing (LSTM-HC) models, REINVENT, JANUS, and a graph-based genetic algorithm (GB-GA). After the algorithm evaluation, they proposed six benchmarks based on the properties of the HOMO–LUMO gap, LUMO energy, molecular dipole moment and PCE, and put forward more detailed function combinations of these properties. According to these benchmarks, they designed a small organic donor and an acceptor molecule to be used in bulk heterojunction devices with [6,6]-phenyl-C61-butyric acid methyl ester (PCBM) and poly [*N*-90-heptadecanyl-2,7-carbazolealt-5,5-(40,70-di-2-thienyl-20,10, 30-benzothiadiazole), respectively. Although these benchmarks should not be viewed as the final performance judgments of any method used (design issues should be case by case), they can still provide preliminary insights. They also claimed that there is currently no champion algorithm capable of performing tasks on all benchmarks.

To date, *de novo* molecular design using deep learning still has much room for improvement. More advanced algorithms, broader and more comprehensive datasets, and more sophisticated guidance for design models are worthy of further consideration by researchers. Also, automated synthesis of molecules is currently a hot topic in high-throughput screening.[79,80] In the near future, we believe that a series of on-demand designs for automated design and synthesis should take chemistry to the next level.

3. Perovskite

Perovskite was named after the Russian geologist Lev Perovski, and initially, it only referred to $CaTiO_3$.[81] Because of the

© 2023 The Author(s). Published by the Royal Society of Chemistry

Open Access Article. Published on 24 April 2023. Downloaded on 2/11/2026 2:23:30 PM. This article is licensed under a Creative Commons Attribution-NonCommercial 3.0 Unported Licence.

development of a class of compounds with the same structure as $CaTiO_3$ (ABO_3), crystal structure compounds with perovskite-like structures can also adopt this first name as a general title. Perovskite is a face-centered cubic structure of the cubic crystal system, and many different cations can be embedded in this structure, allowing the development of a variety of engineered materials.[82–84] This material has been successfully used as a photovoltaic adsorber (usually in a form of perovskite halides),[85] and has the superiority of a high light absorption coefficient, tunable bandgap, high defect tolerance, and simple synthesis method. In recent years, the power conversion efficiency of perovskite solar cells has reached 36%.[86] Owing to the outstanding performance, the perovskite materials have a wide range of applications in a variety of other optoelectronic and energy devices, including (but not limited to) light-emitting diodes,[87,88] catalysts,[89,90] batteries,[91,92] photodetectors, *etc.*[93,94]

3.1 Features and descriptors

There are a lot of features that can be derived from the perovskite structure.[95] In the perovskite structure, the topology of the crystal lattice constrains the positions of the atoms such that the relative positions of the A, B, and O atoms or ions are fixed. This means that when determining the available perovskite structure, researchers can mainly focus on the matching of the dimensions of the A, B, and O atoms. To evaluate the tolerance of ion size mismatch in perovskites when forming different structure types, Goldschmidt introduced a tolerance parameter t calculated from the A, B, O ionic radii ratio, which has been widely applied to study different structures of perovskite.[96] Besides, the octahedral-factor pair μ is also from the basic perovskite structure calculated from the ratio between the ionic radii of anions and cations.[97] With the development of structure research and more datasets for perovskites, the tolerate factors have improved. Bartel *et al.* proposed a new tolerance factor that can be applied to 576 types of materials, achieving a 92% accuracy in classifying whether the materials are perovskites or not.[98] Lu *et al.* enhanced the tolerate factor and octahedral factor, which can cover almost all geometric elements of structural formability.[99] Generally, these two descriptors are widely used not only in computation but also in experiments and their revised version is successfully employed in perovskite machine learning.[100,101]

There are other common descriptors besides the structural features that can be used to represent perovskites, such as atomic, element level properties and macroscopic measurement properties. After considering the A-sites and B-sites, a huge number of microscopic descriptors can be extracted from the atom, such as atom mass, radius, electron affinity, Pauling electronegativity, *etc.* Similarly, macroscopic properties such as density and volume, and space groups can also be included in the feature input. Li *et al.* built a perovskite bandgap energy prediction model, which uses five structure relative factors (such as the tolerance factor) and an initial atomic feature set with 77 atomic physical, chemical and spatial properties.[102] Isayev *et al.* proposed a concept of property-labeled material fragments (PLMFs), which combined the geometry structure with atom/element properties, including the multiplication and ratio of general element/atomic values, measured values and derived properties.[102] Generally, it is possible to use different combinations of descriptors to create new descriptors using expert knowledge. Additionally, a data-driven method such as sure independence screening and sparsifying operator (SISSO) can also be used in exploring new descriptors. To be more specific, SISSO is a math model that is based on the LASSO approach. With the input of physical quantities, it could perform linear combination (unary or binary operators), which can select the best descriptor from a large space of parsed expressions (potential features).[103,104] Many examples show that this method can produce numerous novel descriptors.[105] Usually, using SISSO is accompanied by feature engineering (such as generating several potential descriptors and selecting the most suitable one). For example, Xie *et al.* used the SISSO with atomic radius, valence, electronegativity, permittivity, and nine operators to yield over 182 million descriptors (equations).[106] Finally, after cross-validation, they selected the best features and successfully adopted them in octahedral tilting prediction with 81.7% accuracy. Notably, it is not a fact that the prediction result is better with more combinations of material properties. It is a problem that requires a tailored approach to feature selection. Xu *et al.* showcased that for predicting the properties of ferroelectric perovskites, the traditional machine learning workflow can perform better than the SISSO based method in specific surface area, bandgap, Curie temperature prediction.[107] Therefore, in the choice of material electronic descriptors, multiple explorations can be used to find the optimal solution.

With the development of deep learning, a number of descriptors have been integrated to fit the DL input, which brings a new development in this area.[108,109] Chen *et al.* proposed a novel neural network materials graph network (MEGNet) and represented a series of crystal perovskite structures as graphic structures.[110] To be more specific, as shown in Fig. 6, they followed the GNN normal representation and defined the V, E, and U as atomic (node/vertex), bond (edge), and global state attributes, respectively. The original graph structure information is first updated from the original bond states to the new bond states. Subsequently, the atomic states are updated based on the previous state and bond states. Finally, a new graph structure is generated after using the previous global states. The previous steps are repeated in a cycles until the final result is achieved. 11 of the 13 properties predicted in MAE were under the generally accepted thresholds of chemical accuracy and better than the previous work using the QM9 database. This method also extends to predict the synthesizability and bandgap of perovskites.[111,112]

Besides, automatic unsupervised learning methods can extract hidden information from the original input in the field of perovskites, leading to the formation of non-manual defined descriptors.[113] From an encoding–decoding model such as variational autoencoders (VAE), original features are embedded into a series of compressed latent vectors, which can capture more in-depth features. Using the features extracted only from its chemical formula in the VAE model, Ihalage *et al.* defined the mean vector generated from VAE (μ) as the perovskite material fingerprint (Fig. 7).[114] Furthermore, they verified this

Open Access Article. Published on 24 April 2023. Downloaded on 2/11/2026 2:23:30 PM.
This article is licensed under a Creative Commons Attribution-NonCommercial 3.0 Unported Licence.

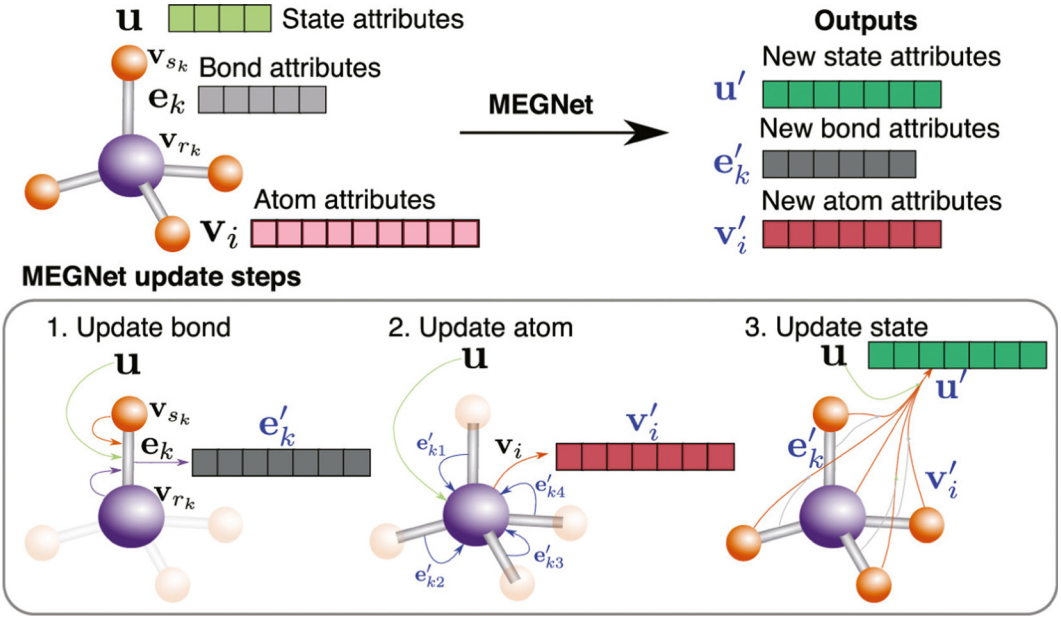

Fig. 6 Overview of a MEGNet module, this figure shows how a graph represents a molecule in the MEGNet. The node attributes fall into three categories: bond, atom, and state. This figure also shows the updating steps in the MEGNet.[110] Reprinted (adapted) with permission from ref. 110. Copyright 2019 American Chemical Society.

new fingerprint with the k-nearest neighbor method and found that in the fingerprint space, similar materials are located close to each other. 5-Nearest neighbors (5-NNs) can determine the correct experimental crystal system of the parent composition with a success rate of 71.8%. Furthermore, non-manual defined descriptors can be used to *de novo* design the perovskite. Based on the generative adversarial network (GAN) and transformer models in machine learning, Dan *et al.* and Wei *et al.* proposed material design models named MatGAN and crystal transformer.[115,116] Wei *et al.* compared these two models and

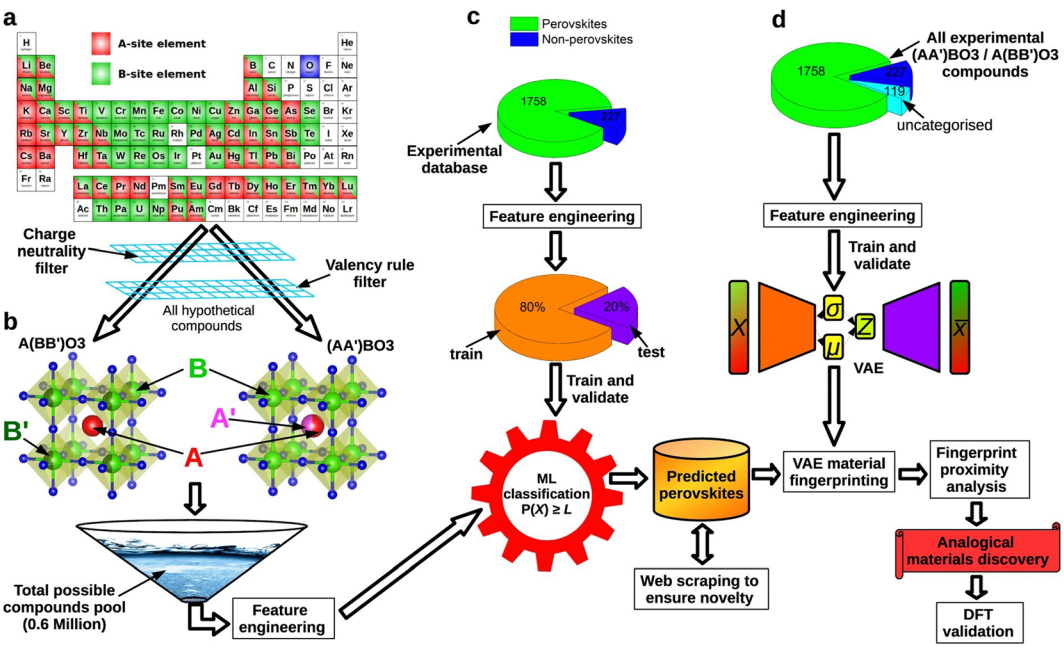

Fig. 7 An overview of using VAE to make perovskite material fingerprints. (a and b) In the part of descriptor creation section, they explored the periodic table for elements that may fully or partially fill octahedral and interstitial positions and specified the following conditions: (1) in the generation, the average oxidation of site A should not be larger than that of site B; and (2) the average ionic radius of the A site should be more than or equal to the average ionic radius of the B site. (c and d) In the model training section, they trained the VAE model on over 2000 unlabeled experimental data sets. Calculation of Euclidean distances in fingerprint space between experimental components and potential perovskites.[114] Reproduced from ref. 114 under the terms of the Creative Commons CC BY license.

© 2023 The Author(s). Published by the Royal Society of Chemistry

Open Access Article. Published on 24 April 2023. Downloaded on 2/11/2026 2:23:30 PM. This article is licensed under a Creative Commons Attribution-NonCommercial 3.0 Unported Licence.

found that the transformer-based model is more suitable for exploration in known chemical spaces due to its ability to capture element interrelationships, whereas the GAN-based model is more appropriate for discovering new molecules in uncharted chemical spaces.

3.2 Types of perovskite prediction tasks

Despite the rapid development of perovskites in recent years, there are still several challenges that restrain perovskite industrialization.[117,118] The first challenge is the requirement of potential new materials. Although lead-based halide perovskites currently have the highest PCE, their decomposition can lead to significant environmental concerns. However, non-lead halide perovskites have not been able to surpass lead-based perovskites in terms of efficiency currently, making it necessary to predict the PCE of materials using computational methods. Additionally, in experimental processes, it is common to judge whether a structure belongs to a perovskite structure or not, and find out how its physical properties (*e.g.*, lattice constant, bandgap, lattice constant, *etc.*) can be regulated. These processes are time-consuming and need a series of experiments. Besides, some kinds of perovskites decompose rapidly in the presence of water vapor, light, increased heat, *etc.*, which deviate from laboratory conditions. Machine learning can play a crucial role in addressing these challenges. Using the trained prediction models, researchers can make rapid and accurate analyses of perovskite structures and physical properties.

Predicting the basic physical information of perovskites can be of great help in the exploration of new materials, the mapping of experimental parameters and the understanding of structure–function relationships. Many models have been developed to predict the physical properties of perovskites such as bandgaps,[109,119] oxide ionic conductivity,[120] thermodynamic stability,[121,122] dielectric breakdown strength,[123,124] lattice parameters,[125] crystal structures.[126] For example, Zhang *et al.* established a model to predict lattice constants based on cubic perovskites.[127,128] Besides, Li *et al.* predicted formation energy, thermodynamic stability, crystal volume and oxygen vacancy formation energy using a variety of machine learning models.[129] Saidi *et al.* constructed a convolutional neural (CNN) model for deriving relevant physical properties (*e.g.*, lattice constants, octahedral tilt angles, *etc.*) from the given perovskite material.[130] Compared to the first-principle methods such as density functional theory (DFT), these kinds of machine learning models can be used for low-cost large-scale screening of physical properties in perovskite materials.

A significant concern in perovskite research is the exploration of identifying potential perovskite structure types. This includes determining which elements can form perovskites and understanding the different structural and compositional variations that are possible within the perovskite structure.[131,132] Many models are successfully established in different kinds of perovskites.[133–135] Taking the electrical and geometrical factors into account, machine learning models established by Li *et al.* were used to predict the formation of perovskite structures and showcased 96.55% and 91.83% accuracy in the single and double perovskite databases.[136] Combining first-principles calculations and machine learning, Talapatra *et al.* proposed to use energy above full = 50 meV as a threshold criterion for database stability and non-stability for perovskite screening.[137] Based on 68 elements from the periodic table, they built a virtual database of 437 828 stable perovskite structures. Based on SHAP analysis, Zhang *et al.* proposed that the formation of hybrid organic–inorganic perovskite (HOIP) structures is more likely to occur when the A site radius falls within the range of 1.95–3.25 Å and the B site radius falls within the range of 0.60–1.20 Å[138] Besides, machine learning can also be adopted in identifying the perovskite structure in experimental characterization. Massuyeau *et al.* built RF/CNN models capable of identifying XRD peaks using XRD diffraction patterns as the training set, which can directly distinguish between perovskite and non-perovskite materials.[139] All of these works provide good paradigms for identifying perovskites.

Searching for the stability and high PCE lead-free halide perovskites[140] is also an important downstream task of perovskite machine learning application. Using the property density distribution function (PDDF), Stanley *et al.* constructed features and applied them to predict the bandgap, formation energy, and convex hull distance of lead-free halide perovskites.[141] Besides, machine learning can also be used in the design of new types of lead-free halide perovskites. Lu *et al.* reported a HOIP prediction model trained from 212 reported bandgap values.[142] Using a combination of DFT optimization and machine learning prediction, they determined the range of tolerance factors, octahedral factors, metal electronegativity, and polarizability of potentially promising HOIP organic molecules and selected 3 thermal and environmental stable lead-free HOIPs with appropriate bandgaps from 5158 candidates. In addition, there have been research efforts that combine machine learning and DFT,[143] for discovering lead-free hybrid perovskite,[144] two-dimensional lead-free perovskite[145] and others.[118,146] These works provide a solid foundation for discovering more efficient and stable lead-free halide perovskites.

One of the major challenges that remains to be addressed in perovskite applications is the stability of devices. The stability of the perovskite devices falls short of mainstream silicon devices. Odabas *et al.* analyzed the hysteresis and reproducibility of perovskite solar cells and proposed materials and alternatives for perovskite deposition with low hysteresis and high reproducibility.[147] In materials, in addition to thermodynamic stability, another more important aspect to consider is mechanical stability (or mechanical strength). Jaafreh *et al.* investigated the mechanical strength of perovskite-based materials using the AdaBoost algorithm with the volume and shear quantities of the elastic modulus and its scaling criterion (satisfying G/B smaller than 0.57 for ductility at room temperature (RT)). Based on the model, they identified about 770 perovskites with mechanical strength.[148] Howard *et al.* proposed a reap-rest-recovery (3R) cycle machine learning framework to avoid permanent failure of perovskites due to exposure to water vapor and oxidation.[149] Due to the complexity of factors such as device stability, more effective models with interpretability still need to be developed for evaluation to help find a suitable device.[150]

Open Access Article. Published on 24 April 2023. Downloaded on 2/11/2026 2:23:30 PM.
This article is licensed under a Creative Commons Attribution-NonCommercial 3.0 Unported Licence.

Compared with using virtual datasets, using real-world datasets is considered a more appropriate approach for predicting the properties of perovskite materials. However, one of the obstacles of this method is the time-consuming and labor-intensive process of manually collecting and cleaning large datasets from thousands of perovskite-relevant articles. Thanks to the development of natural language processing (NLP), much of the chemical text and information extraction toolkits are proposed such as ChemDataExtractor, OSCAR4, ChemicalTagger and others.[151–154] Thus, it is possible to do text mining and build relatively large real-world datasets for perovskite prediction.[155,156] Beard *et al.*[157] adopted the ChemDataExtractor to build two datasets from 25 720 articles regarding dye-sensitized solar cells (DSCs) and perovskite solar cells (PSCs).[157] Furthermore, using an automatic collection dataset can directly train the machine learning model. Kim *et al.* proposed a linguistic model-based approach for linking the scientific literature to material synthesis insights and successfully performed perovskite synthesizability screening (prediction of two precursors).[158] Although there are few examples in the area of text-mining, it is likely that in the future the text-mining method will play an important role in building perovskite datasets as the amount of scientific literature data continues to grow.

3.3 Experimental conditions and acceleration

In many cases, machine learning is often used as a powerful tool for experiment-free exploration in perovskite research. Although decision trees and SHAP's interpretable mechanisms can provide an intuitive understanding of how a model arrived at its predictions, it is not always clear if the underlying assumptions of the model are valid or if they accurately represent real physical processes. One explanation is that the experimental environment is usually more complex than the features input in the machine learning models.[7,159] Additionally, data from different articles may be collected under different conditions, using different measurement techniques, or with different levels of measurement accuracy, making it difficult to compare and use in a machine learning model. It is important to validate the accuracy of machine learning models by combining the results of machine learning calculations with experimental work.[160] This approach helps to ensure that the predictions made by the models are accurate and reliable. By using machine learning as a tool, it is also possible to accelerate perovskite

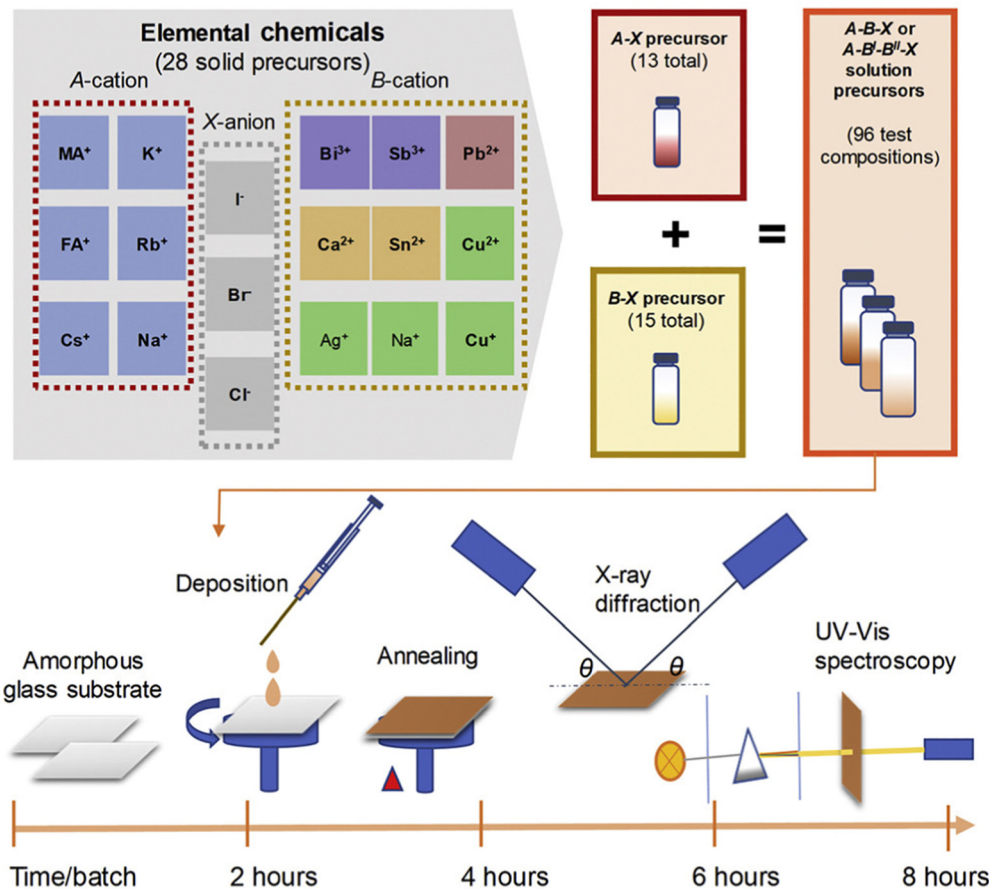

Fig. 8 High throughput experiments conducted by Sun *et al.* Precursor solutions were prepared and a high throughput experimental cycle was designed. Three experiments and characterization were carried out to examine the structural and optical properties according to thin film deposition, X-ray diffraction and UV-visible spectroscopy.[161] Reprinted (adapted) with permission from ref. 161. Copyright 2019 Elsevier.

© 2023 The Author(s). Published by the Royal Society of Chemistry

Open Access Article. Published on 24 April 2023. Downloaded on 2/11/2026 2:23:30 PM.
This article is licensed under a Creative Commons Attribution-NonCommercial 3.0 Unported Licence.

discovery experiments in real-world conditions (usually with high throughput experiments)[161,162] (Fig. 8). All of these works are considered as accelerating the speed of the experiments.

To be more specific, the accelerated experiments assisted by machine learning can be divided into two parts, to explore the experimental condition and realize verification.[163] In the aspect of materials or experimental reagent selection, there are a lot of studies that have been reported. Yu *et al.* used machine learning to study the reactivity trends of different types of amines and suggested five property recommendations of amines for post-treatment of $MAPbI_3$.[164] By developing the capping layer, Hartono *et al.* used RF regression and SHAP values to find the features having the largest contribution to stability, and found that the most important properties for prolonging the onset of degradation were a low number of hydrogen bond donors and a small topological polar surface area.[165] Furthermore, based on their model, they proposed and experimentally validated phenyltriethylammonium iodide (PTEAI) as the best capping layer material. They found that the stability lifetime of $MAPbI_3$ was 4 ± 2 over bare $MAPbI_3$ and 1.3 ± 0.3 over octylammonium bromide (OABr), which is SOTA at that time. They also gave a corresponding explanation based on XPS and FTIR results that the capping layer on top stabilizes $MAPbI_3$ by changing the surface structure and chemistry, which match the previous experiment regulations.[166,167] Besides, by machine learning and experimental verification, Cai *et al.* confirmed the ratio of Sn: Pb in $MASn_xPb_{1-x}I_3$ holding an Sn–Pb alloy within the perovskite crystal.[168]

In exploring the device stability condition part, Hu *et al.* investigated the factors affecting the stability of perovskite solar cell devices through a combination of experiments and machine learning.[169] Five factors affecting the efficiency and stability (grain size, defect density, bandgap, fluorescence lifetime and surface roughness) were selected using machine learning models and proposed that roughness and crystal size have a strong influence on long-term stability. Subsequently, based on a self-built PCE model, they designed different conditions to vary the surface roughness to achieve the best stability of perovskite devices at 25% humidity and 25 degrees Celsius.

Machine learning-assisted high throughput experiments for automated synthesis have an important role in replacing manual synthesis and a large-scale exploration of perovskites.[170–172] More specifically, human-based operations are replaced with fully automated robotic working and the process is iterative between automated experiments and machine learning-based experiment planning. This method can speed up the experiment considerably compared to human labor. For example, Li *et al.* reported a high-throughput robotic perovskite synthesis system that takes 20-fold less time than manual synthesis.[173] Bayesian optimization is the most commonly used algorithm, which performed well in low-dimensional parameter space.[174,175] As shown in Fig. 9, MacLeod *et al.* developed an 8-step thin film modular robotic platform called 'Adad', which automatically synthesizes, processes, and characterizes thin-film samples. Using ChemOS in the previous work, a Bayesian optimization

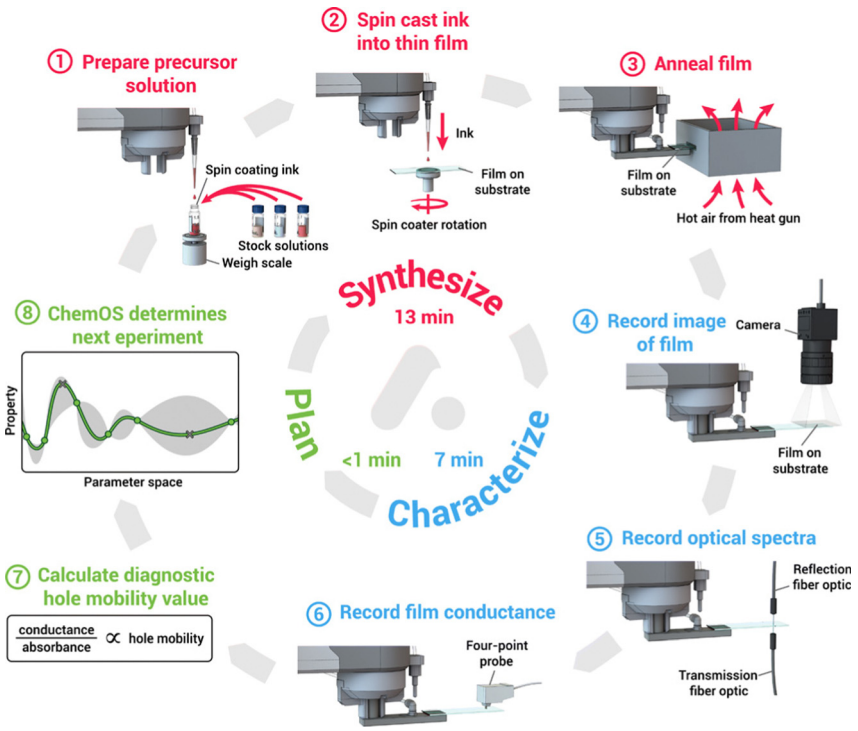

Fig. 9 8-Step auto-platform combining synthesis, characterization, software machine learning calculation into a self-driving workflow to make thin film samples, this work reported by Macleod *et al.*[176] Reproduced from ref. 176 under a Creative Commons Attribution NonCommercial License 4.0 (CC BY-NC).

© 2023 The Author(s). Published by the Royal Society of Chemistry

Open Access Article. Published on 24 April 2023. Downloaded on 2/11/2026 2:23:30 PM. This article is licensed under a Creative Commons Attribution-NonCommercial 3.0 Unported Licence.

algorithm was applied to design the next sample for the experiment after the characterization.[176,177] Besides, Higgins *et al.* used a pipetting robot to build a perovskite combinatorial library and used Gaussian regression (a form of Bayesian optimization) to analyze the physical properties of the constituent series.[178] However, compared to the integrated pervasive API interface of machine learning, machine learning-assisted high-throughput experiments still require the development of a pervasive experimental system and software in the future.

4. Machine learning in catalytic reactions

Catalysis is important in energy storage systems.[179,180] Catalytic reactions are complex due to multi-phase involved surfaces/interfaces, mass transfer effects, and various geometric/electronic structures of catalysts.[181–187] Traditional methods for designing catalysts mainly focus on synthesis and computational-assisted design, hoping to understand the mechanisms and derive empirical rules for catalytic properties. However, it is greatly limited by the quality of experiments and the precision of calculations. Machine learning helps researchers to have a better understanding of the structure–property relationships and accelerate the discovery of new catalysts.

4.1 Optimizing potentials

Machine learning is a powerful tool for optimizing interatomic potentials. Traditionally, a lot of physics-based potentials have been applied to Monte Carlo simulations and molecular dynamics (MD) simulations.[188–191] However, the accuracy of these potentials cannot be guaranteed and is hard to improve. First-principles simulation can provide enough accuracy, but it is limited by the cost of calculations. It is impossible to run enough first-principles calculations for different types of potentials. With the development of machine learning, it becomes possible to train models with a practical number of first-principle calculations and obtain accurate atomistic potentials. This routine would accelerate MC/MD calculations and allow for long time scale simulations.[192,193]

By using machine learning methods, machine learning potentials are obtained by fitting energy and force from DFT calculations. A classical method was proposed by Behler and Parrinello in 2007.[194] Similar to empirical potentials, the total energy E could be expressed as a sum of atomic contributions E_i, an approach that is typically also used in empirical potentials.

$$E = \sum E_i \tag{1}$$

In Behler *et al.*,[194] researchers proposed a neural-network (NN) representation of DFT potential-energy surfaces (PESs). The advantage of this method is that it could provide the energy and forces of all atomic positions, which is faster than first-principle methods and applicable to both periodic and nonperiodic systems. The critical point is the introduction of a new symmetric function, where each atom reflects the local environment that determines its energy. Furthermore, Behler improved this symmetry function in 2011, which is called the atom-centred symmetry function (ACSF).[195] The inspiration is that Cartesian coordinates are not good enough to represent atomic positions. So a transformation to symmetry functions is necessary to construct high-dimensional NN PESs. This method is applicable to different types of systems, like molecules, crystalline, amorphous solids, and liquids.

Another important method to calculate PESs was proposed by Bartok *et al.*,[196] in which a kernal-based descriptor was applied. In this research, they started with forming a local atomic density related to neighbor atoms, and converted the PES to an interpolation of the atomic energy in the truncated bispectrum space. By using Gaussian process (GP) regression, they realized a good approximation to the atomic energy function. Then with different sparse configurations, they proposed a final expression called the Gaussian approximation potential (GAP) model. This model also performs well in bulk crystals at high temperature. As a typical method, it has been applied to develop smooth overlap of atomic positions (SOAPs).[197] This proves that some widely used descriptors could be concluded using a general approach, where they applied a finite set of basis functions to expand the atomic neighborhood density function. To make a best estimate of atomic energy function, it assumes a Gaussian basis function as below:

$$\varepsilon(b) = \sum_n \alpha_n e^{-(1/2)\sum_l [(b_l - b_{n,l})/\theta_l]^2} = \sum_n \alpha_n G(b, b_n), \tag{2}$$

where n and l range over the reference configurations and bispectrum components, respectively, and θ_l are (hyper) parameters.

Thompson *et al.*[198] proposed a new interatomic potential for solids and liquids, which is called spectral neighbor analysis potential (SNAP). Different from the GAP model proposed by Bartok,[196] researchers proposed the bispectrum as its descriptor and assumed a linear relationship between atom energy and bispectrum components. In SNAP, the coefficients are determined by the weighted least-squares linear regression, which allows the model to fit a full set of quantum mechanics calculations. Also, the symmetry properties are applied to reduce the computational cost.

By utilizing graph convolutional neural networks (GCNNs), Schutt *et al.*[199] developed a deep learning architecture SchNet to model atomic systems. By using continuous-filter convolutional layers, SchNet is able to predict the potential-energy surfaces and energy-conserving force fields of small molecules, which could be utilized in MD simulations. Also, GCNN has been applied to overcome the limitations of traditional methods, which do not consider the spatial information. Gasteiger *et al.*[200] constructed a directional message passing neural network (DimeNet) that embeds the messages passed between atoms by considering directional information.

A deep learning method is promising in promoting the efficiency of calculating many-body potential energy. Zhang *et al.*[201] designed a DeePMD-kit to build potential energy and

© 2023 The Author(s). Published by the Royal Society of Chemistry

Open Access Article. Published on 24 April 2023. Downloaded on 2/11/2026 2:23:30 PM. This article is licensed under a Creative Commons Attribution-NonCommercial 3.0 Unported Licence.

force fields by using deep learning methods. The model used a function containing coordinates and elemental types as descriptors. By training the data from the AIMD to DeePMD model, the MD stimulations can accurately replicate the results of the original AIMD data. The DeePMD-kit is written with Python/C++ and interfaced with TensorFlow, which improves the training efficiency and user-friendly.

Also, a lot of software packages have been used to build deep learning potential energy surfaces. The promotion and application of machine learning models greatly benefits the development of atomistic potentials, as we listed several typical packages in below: 1. LASP:[202] learning-based atomistic simulation package (LASP) is a software platform that merges the stochastic surface walking (SSW) method and global neural network (G-NN) potential for exploring and evaluating the PES. LASP provides various simulation techniques for PES data building, exchange, and G-NN potential generation within a single platform. 2. AMP:[203] the atomistic machine-learning package (AMP) is a software package for building and using machine learning models for atomistic simulations. It is designed to handle large-scale simulations and includes features for parallelization and incorporating diverse training data. 3. SchNetPack:[204,205] SchNetPack is an open-source software package for building neural network potentials for molecular and material simulations. It includes a variety of NN architectures, as well as tools for generating and analyzing training data. 4. MLIP:[206–208] the machine learning interatomic potentials (MLIP) software package is a Python library for building interatomic potentials using machine learning models. It includes a variety of machine learning algorithms, as well as tools for generating and analyzing training data.

In conclusion, machine learning has been widely applied to find the PESs and atomic forces. With the development of machine learning algorithms, different descriptors and regression methods have been applied, leading to great progress. Compared with *ab initio* calculations, adopting machine learning could largely reduce the computational cost and maintain acceptable accuracy. It is promising to apply machine learning methods in MD/MC calculations.

4.2 Predicting catalytic ability

A lot of models and descriptors have been proposed to describe the catalytic activity. Among them, the d-band center theory is a classical descriptor for describing the relationship between the adsorption intensity and the energy of d-band center, which leads to different catalytic activities.[209] However, calculating the d-band center of metals by applying the first-principles methods consumes a lot of CPU time. So it is convenient to predict d-band centers by using machine learning tools. Takigawa *et al.*[210] compared with different regression models and applied the gradient boosting regression (GBR) method with six descriptors to predict the d-band center of 11 metals and their pairwise alloys. The result shows a reasonably accurate d-band center energy with an average root mean square error (RMSE) <0.5 eV.

Adsorption decides the interaction intensity between active intermediates and the catalyst, and overpotential determines the behavior when assembling catalysts in batteries. Lian *et al.*[211] investigated single-atom catalysts (SACs) for lithium–sulfur (Li-S) batteries. At first, researchers classified the adsorption process by the presence or absence of S–S bond breaking. Then, crystal graph convolutional neural network (CGCNN) was applied to complete the classification and regression.[212] By obtaining 812 adsorption configurations on 203 SAC catalysts, researchers categorized them into 4 categories and excluded unstable catalytic configurations. After training the machine learning model, its prediction has a mean absolute error of 0.14 eV (Fig. 10a). As shown in Fig. 10b, for different elements, researchers calculated two elementary steps and plotted their free energy as ΔG_1 and ΔG_2. These two elementary steps were identified as potential limiting steps depending on the LiS* adsorption energy, which shows a volcano plot as shown in Fig. 10c. And by calculating the overpotential for different metal sites and supporter composites (Fig. 10d), researchers concluded that higher overpotential would lead to a limited catalytic activity. Based on the volcano plot and overpotential results, it could be applied to optimize the synthesis of SACs and predict catalytic activities.

The oxygen reduction reaction (ORR) and oxygen evolution reaction (OER) are key reactions for fuel cell and metal–air batteries.[213–216] The ORR/OER are limited by 4 electron transfer and sluggish kinetics, so it is important to design efficient electrocatalysts for these two reactions. In recent years, SACs have been widely applied in the ORR/OER, and achieved high activities.[217–219] And this has led to increased interest in investigating the key factors for these reactions, which could assist in understanding the mechanism. Ying *et al.*[220] found a volcano-shaped relationship between the catalytic activity and ΔG_O, and applied machine learning model based on the RF algorithm. With consideration of the scaling relationship and the feature importance, it determined the outer electron number and oxide formation enthalpy as the two most important factors. And the machine learning model could give an accurate prediction of ΔG_O efficiently.

Furthermore, SACs still have some limitations, like compatible low stability and simple adsorption configurations. So researchers further introduced dual-metal-site catalysts (DMSCs),[221,222] which could both enhance the activity and optimize surface adsorption. The increase in metal sites also increases the difficulty of investigating specific factors that contribute to reaction activity. So machine learning methods have been applied here to reveal the order of important factors,[223] which benefits the optimization of catalysis design.[224,225]

Zhu *et al.*[226] conducted DFT calculations to calculate the adsorption free energy and screen high ORR activity DMSCs as the flowchart shown in Fig. 11a. By training models based on the GBR algorithm,[227] it showed a low RMSE of 0.036 eV. And mean impact value (MIV) has been applied here as an indicator to assess the importance of features. With this tool, researchers proposed 7 features that were mostly related to the catalytic activity of DMSCs, and determined that the electron affinity of metal atoms is the most important feature for the activity of DMSCs. This result provides a valuable insight for synthesizing DMSCs.

Open Access Article. Published on 24 April 2023. Downloaded on 2/11/2026 2:23:30 PM.
This article is licensed under a Creative Commons Attribution-NonCommercial 3.0 Unported Licence.

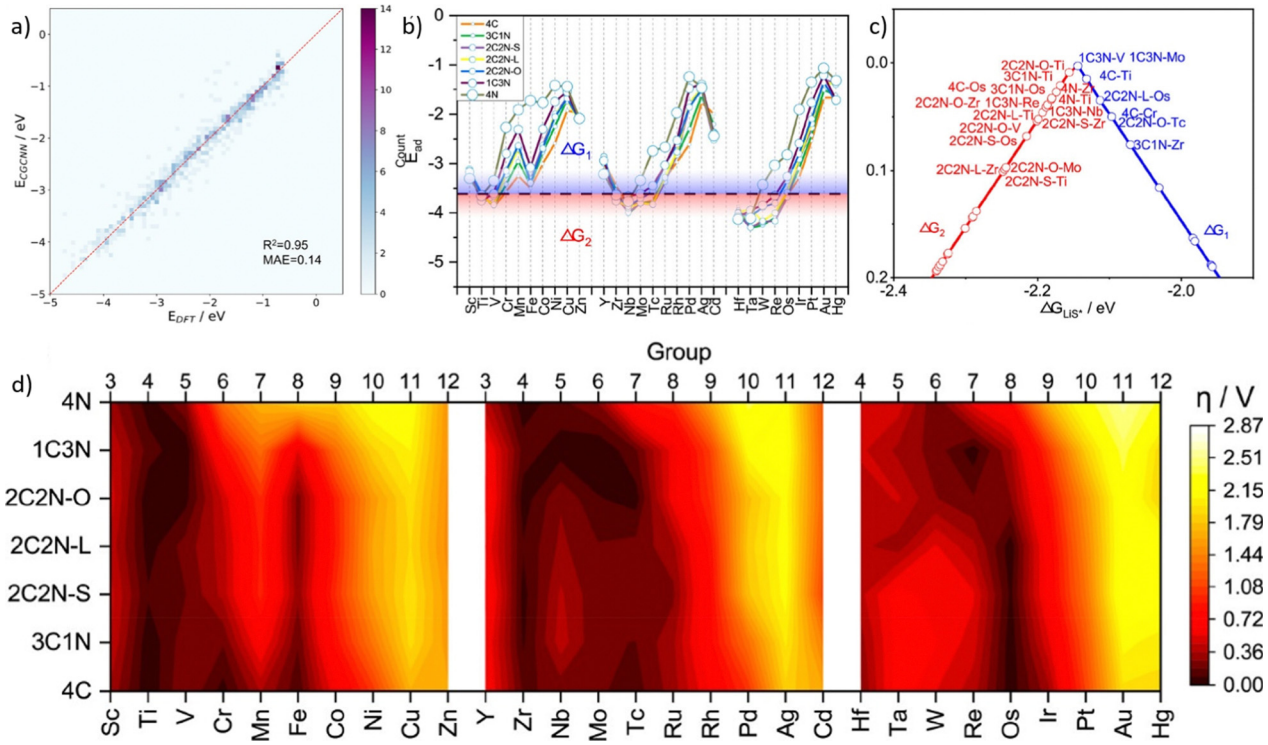

Fig. 10 Taken from Fig. 3 and 4 in Lian *et al.*[211] (a) DFT calculated and machine learning predicted adsorption energy of Li-polysulfides, (b) predicted adsorption energy of LiS*, (c) volcano plots for catalysts with an overpotential lower than 0.1 V, and (d) heat map of the predicted overpotential of different SACs. Reproduced with permission.[211] Reprinted (adapted) with permission from ref. 211. Copyright 2021 American Chemical Society.

5. Machine learning in batteries

Since the first commercial product came out in 1991, Li-ion batteries have been developed for over 30 years. As some of the most promising energy storage devices, they have wide applications in vehicles, electronic devices, and aerospace.[228–230] The focus of development of Li-ion batteries is on the energy density, lifetime, and safety. To solve the bottlenecks in practical applications, it is important to design and optimize different parts of batteries. Currently, Li-ion batteries are suffering from low coulombic efficiency, poor electrode stability, and formation of dendrites.[231–235] Researchers put a lot of effort into developing electrodes, electrolytes, and battery management systems to avoid these issues.

A lot of effort has been made in finding new chemistry in battery electrodes, and electrolytes. However, each material has different electrochemical properties, and it is hard to optimize directly. With the development of machine learning, it becomes a powerful tool in dealing with complex factors and provides relationships between structure and their functions. Machine learning assists the design of batteries and boosts the discovery of energy storage materials.

5.1 Predicting electrode materials

For Li-ion batteries, electrode materials play a crucial part in determining voltage, capacity, Li storage ability, and stability of the structure and cycling.[236–240] It is important to predict these

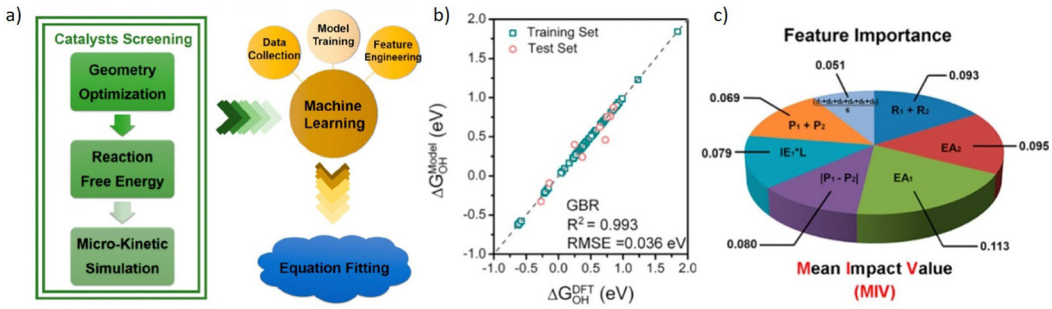

Fig. 11 Taken from Fig. 4 by Zhu *et al.*[226] (a) Schemetic plot of screening high efficient DMSCs from DFT calculation and trained with the machine learning model, (b) training results of ΔG_{OH}, (c) feature importance based on the MIV. Reproduced with permission.[226] Reprinted (adapted) with permission from ref. 226. Copyright 2019 American Chemical Society.

© 2023 The Author(s). Published by the Royal Society of Chemistry

Open Access Article. Published on 24 April 2023. Downloaded on 2/11/2026 2:23:30 PM.
This article is licensed under a Creative Commons Attribution-NonCommercial 3.0 Unported Licence.

properties based on the intrinsic properties of electrode materials. And finding a clear structure–function relationship would benefit researchers to gain insights into the behavior of electrode materials.[241,242] Many machine learning models have been used to predict the properties of battery electrode materials. Joshi *et al.*[243] applied DNN, SVM, and kernel ridge regression (KRR) as algorithms. Then, the model was trained with data taken from the Materials Project database,[244,245] and a voltage profile of electrodes was obtained. By applying a total of 4250 data instances for 3580 intercalation-based electrode materials, researchers extended their predictions to different metal-ions (Li, Mg, Ca, Al, Zn, and Y) batteries. Their results showed a good fit for predicting the voltage of current electrode materials. The machine learning model is also able to investigate new electrode materials by replacing Li with other metals. The result shows a similar trend compared with experimental results.[246]

Besides the voltage of electrode materials, the Li-ion conductivity is also a significant factor that decides the performance of batteries. For different electrode materials, the conductivity can differ in tens of magnitude,[247,248] so how to develop high Li-ion conductivity materials is of great importance. Sendek *et al.*[249] discovered a lot of crystalline solid materials through density functional theory simulations guided by machine learning-based methods. In this research, researchers compared the machine learning guided method with random search of material space, and received at least a 44 times improvement in the log-average of room temperature Li ion conductivity. It is also evaluated from the F1 score, which is 3.5 times better than completely random guesswork and much better than human brains. The screening result shows that most of the high conductivity materials are found by applying the machine learning guided search, which proves its superiority over the traditional guess and test method.

With the development of the Materials Project database, there are a lot of material data that could be utilized for training a machine learning model. However, the quality of models is greatly limited by the quality and quantity of data, and for each material, not all properties are well prepared. So developing an unsupervised learning method is valuable, as it could avoid labeling data and requires less data points. Zhang *et al.*[250] proposed an unsupervised learning model to find materials for solid-state Li-ion conductors. As is shown in Fig. 12a, researchers applied an agglomerative hierarchical clustering method to train a mXRD dataset, and it shows similar characteristics with the real mXRD pattern (Fig. 12b and d), which means a good quality of classification. Then this model was used to find solid-state Li-ion conductors (SSLCs) with high Li-ionic conductivities and group them accordingly. (Fig. 12c). To confirm the superiority of the unsupervised learning, they conducted AIMD simulations, and the result shows that the model discovered 16 new fast Li-conductors with conductivities of 10^{-4} to 10^{-1} S cm^{-1}.

Previous works mainly focused on finding new compounds as electrode materials. Except for screening and designing electrode materials using components, optimizing heterogeneous electrode microstructures is also a powerful tool in designing batteries.[251] Starting from microstructures could unveil the relationship between structures and functions clearly. With the help of machine learning, complex structures could be designed. The reconstruction routine consists of two major strategies, statistical sampling and optimization. A common method is to sample descriptors of different microstructures, and follow up with minimizing the difference between reconstructed structure and real structure. Based on this method, different modeling methods could be applied to build 3D electrode models, like physics-inspired Monte Carlo method and hierarchical reconstruction.[252,253]

5.2 Designing electrolytes

Electrolytes play an important role in Li-ion battery systems, like forming the solid electrolyte interphase (SEI) layer, conducting Li^+, and the compatibility of electrodes.[254–257] A lot of investigations have been made to find new chemistry of electrode materials and reactions, but the research on electrolytes is less. A typical commercial electrolyte is $LiPF_6$ and organic carbonate solvents, as it is easy to operate and cheap.[258,259]

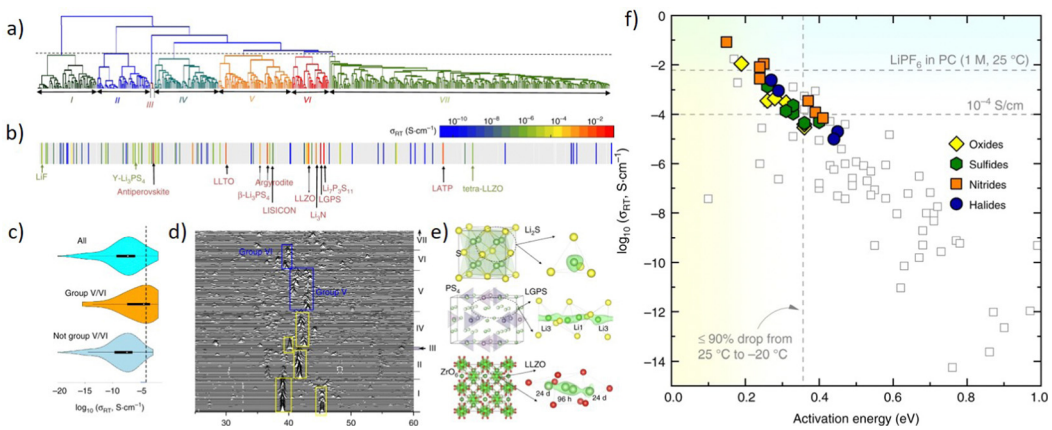

Fig. 12 Plots remade from Fig. 2 and 3 by Zhang *et al.*[250] (a) the tree diagram of the agglomerative hierarchical clustering method, (b) the dendrogram to the conductivity reveals grouping of known solid-state Li-ion conductors, (c) violin plots of σ_{RT} data grouped in the grouping, (d) mXRD of materials, (e) crystal structures (left) and (right) Li sites (green sphere) determined by local anion (yellow/red sphere) configurations, and (f) σ_{RT} *vs.* activation energy, ion conducting properties of newly predicted shown as filled symbols. Reprinted (adapted) with permission from ref. 250. Copyright 2019 Springer Nature.

Open Access Article. Published on 24 April 2023. Downloaded on 2/11/2026 2:23:30 PM.
This article is licensed under a Creative Commons Attribution-NonCommercial 3.0 Unported Licence.

Plus, with the existence of electrolyte additives, it could stabilize the electrolyte skeleton and improve the formation of the SEI. So the design of electrolytes is focused on lifting the ionic conductivity, safety and stability.

Machine learning is a strong tool for large scale screening materials and their properties. Jalem *et al.*[260] proposed a NN method for screening potential solid state electrolyte (SSE) materials. In the research, researchers utilized NN and searched in the $LiMXO_4$ group. The screening was mainly focused on two properties, the Li diffusion barrier and the cohesive energy. These two properties are important for Li-ion conductivity and bonding information. Researchers revealed the relationship between diffusion barrier, the cohesive energy and their structure descriptors in the materials space. Compared with traditional partial least squares, the application of multi-output node architecture could increase the accuracy of prediction.

Also, to realize the finding of new chemistry, the structure–function relationship needs to be investigated carefully. Kireeva *et al.*[261] applied the support vector regression to investigate the composition–structure–Li ionic conductivity relationships. It could be utilized to define parameters that lead to high Li-ion conductivity, and search in a large material space, which could provide potential materials as SSE.

As shown in Fig. 13a, the model predicts the conductivity well with the experimental result. The accurate result could provide a significant insight into the co-doping effect, which is not completely issued by DFT calculation. Generally, the doping of different cations shows the same trend without outlier-by-prediction. Fig. 13b provides a model with an additional descriptor pool. It reveals the impact of different parameters on the property space.

Besides, machine learning could also be applied to predict mechanical properties like the growth of dendrites. Dendrite formation is a serious problem that affects the safety of batteries.[262,263] Using solid electrolytes is a promising method to deduce dendrites, which could suppress the formation of dendrites greatly. Ahmad *et al.*[264] calculated properties of mechanically isotropic and anisotropic interfaces as the criteria of dendrite initiation. Then a GCNN was trained on the shear and bulk moduli, and gradient boosting regressor and kernel ridge regression were used to train the elastic constants. With these machine learning methods, 20 mechanically anisotropic interfaces could be predicted between Li metal and four solid electrolytes as the candidate materials.

SSEs are also promising for addressing the flammability concerns, which requires to form a high quality SSE layer. To evaluate the quality of SSE films, both conductivity and uniformity are considered. Chen *et al.*[265] proposed a high-quality SSE film synthesis method guided by machine learning. In this research, researchers adopted three algorithms (principal component analysis, K-means clustering, and support vector machine) to analyze the relationship between fabricating parameters and film quality. Principal component analysis has been used to determine the manufacturing conditions and converts it to a low dimensional subspace. Then K-means algorithm is applied to classify different films and defines its performance. Finally, a support vector machine unveils the effect of fabricating parameters on the quality of films. When assembling the whole cell, the SSE film shows a good stability, proving this method to be useful. The machine learning-assisted method successfully optimized the production of SSE films.

In conclusion, machine learning boosts the design of electrolytes and screening materials with superior physical properties. Compared with traditional first-principle methods, machine learning methods are able to consider more factors that determine the behavior of electrolytes and directly guide fabrication process in batteries.

5.3 Optimizing battery management

When fabricating commercial products, strict process control and optimization of parameters are important.[266,267] Among all these parameters, how to maximize the lifetime of batteries and monitor the health condition has been considered as an important topic.[267] Traditionally, lifetime testing of batteries needs long term experiments that may last for months.[268] And with a variety of charge/discharge conditions for batteries, it is hard to predict a certain health condition directly. These issues bring trouble for sampling batteries and hinder the selection of

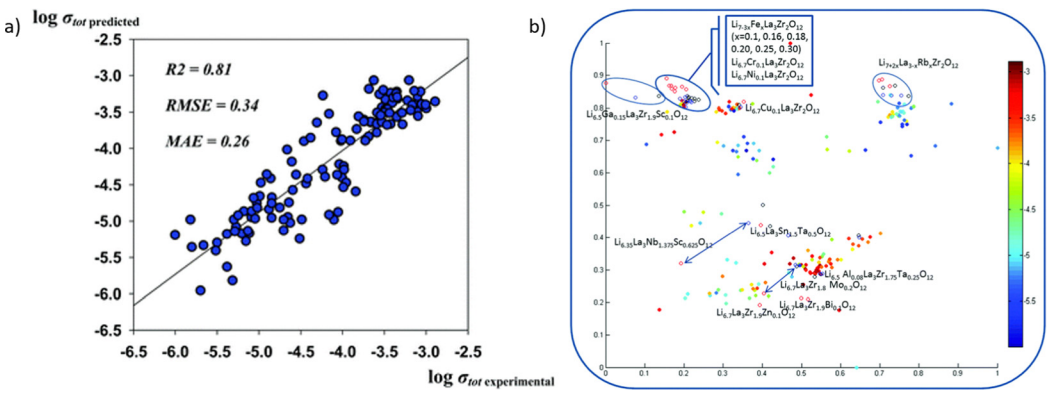

Fig. 13 (a) The prediction accuracy of Li conductivity by machine learning models and (b) the conductivity results categorized using different synthesis methods, and adapt t-stochastic triplet embedding, where experimental results are served as an extra descriptor pool. Reproduced from ref. 261 with permission from the PCCP Owner Societies.

© 2023 The Author(s). Published by the Royal Society of Chemistry

Open Access Article. Published on 24 April 2023. Downloaded on 2/11/2026 2:23:30 PM.
This article is licensed under a Creative Commons Attribution-NonCommercial 3.0 Unported Licence.

representative data. Since machine learning is powerful in data learning and predicting, it is promising to develop advanced algorithms to optimize parameters in batteries and monitoring lifecycles.[269]

To estimate the state of charge and health, it is significant to build efficient models to describe battery management systems. A main battery model that applies in battery systems is equivalent circuit models (ECMs),[270,271] which simplifies complex systems to circuits and fits models. For further advancement, physics-based models (PBMs) are being developed for battery systems,[272] which can take into account multi-dimensional information, like real time scale analysis, and battery dynamic parameters.[273,274] These models are always limited by their complexity and require a large computational source to solve them. With the development of machine learning, a lot of methods and algorithms have been applied to simulate battery systems, including multiple regressions, NN, and Bayesian.[275–277]

An early-prediction strategy has been an important method for predicting the state of health (SoH) and remaining useful life (RUL) of batteries, as it could shorten the time of experiments and improve the efficiency of optimization. As shown in Fig. 14, Attia *et al.*,[278] researchers proposed a closed-loop optimization (CLO) system, combining an early-prediction model and a Bayesian optimization algorithm to accelerate the time of identifying charge protocols. This strategy sampled the first 100 cycles and utilized it as input for a linear model *via* elastic net regression to find charging protocols.[279] Compared with full cycle experiments, the early-prediction model accelerated more than 30 folds. Then, by applying a Bayesian optimization algorithm to early-prediction data, it could provide an optimized result for next-round charging protocols.[280,281] With these two strategies, the article made a successful approximation to the average life cycle and uncertainty of protocols. Also, utilizing early-prediction results reduced the total optimization cost, which is beneficial for the wide application of the CLO system. Furthermore, the early prediction strategy could be extended and integrated with Monte Carlo simulation to predict the battery remaining useful life.[282] Tong *et al.*[282] proposed a deep learning algorithm, named adaptive dropout long short-term memory (ADLSTM). By obtaining early cycle capacity as training data, researchers trained the model, and used long term cycles as testing data. With a trained model, MC is applied to figure out the uncertainty of battery data, and enhanced the robustness of the model. This method showed the lowest errors compared with other algorithms.

As a classical energy storage system, Li-ion batteries have been widely applied in daily life because of their high energy density.[283–285] However, the degradation of Li-ion batteries, due to their complex and non-linear deactivation, has caused a lot of issues for recycling.[286,287] To decide the state of health and remaining useful life of batteries, traditional methods mainly rely on multiscale simulations.[288] But conventional simulation tools cannot perform well on a wide length scale and long time scale. So it is more accessible to combine different characterization and machine learning methods to generate a large amount of data and build an efficient statistical model.

For investigating battery systems, electrochemical impedance spectroscopy (EIS) is a classical method to measure the relationship between input and output, like capacity and resistance.[289] However, it is hard to predict battery properties using EIS since the result of EIS contains both real and imaginary part, and still there are debates on if an electrical model could describe a complex battery system.[290–292] Zhang *et al.*[293] built a battery forecasting system with a GP model. By feeding over 20 000 EIS results of commercial Li-ion batteries, the GP model could predict degradation and remaining useful life successfully. With one of the largest dataset, researchers could estimate the capacity and RUL of batteries

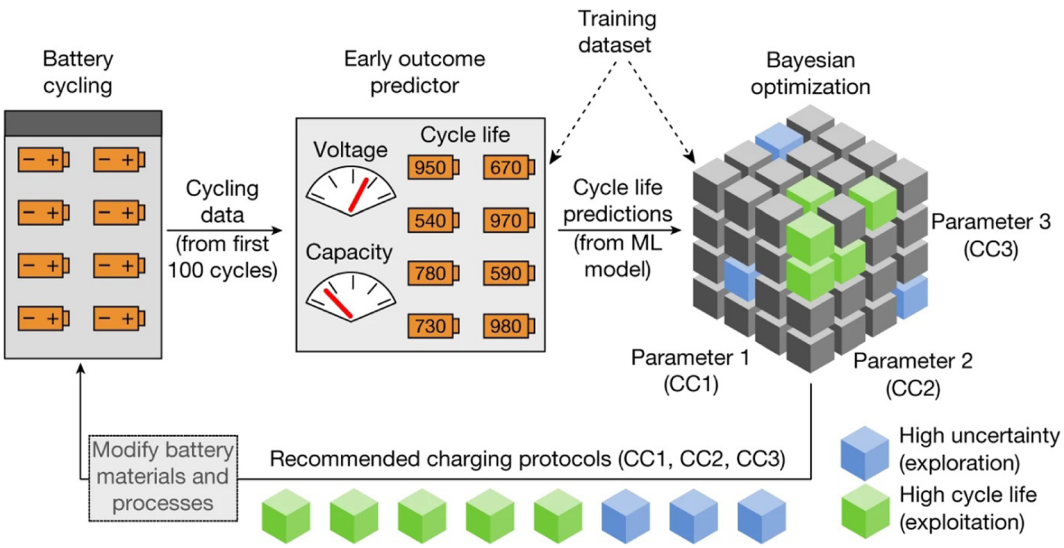

Fig. 14 Schematic plot of the closed-loop optimization (CLO) system applied to predict the cycle life. Researchers adapted the first 100 cycles data as the first feeding data and applied Bayesian optimization to determine parameters. This method provides insights to designing parameters of batteries. Reprinted (adapted) with permission from ref. 278. Copyright 2019 Springer Nature.

Open Access Article. Published on 24 April 2023. Downloaded on 2/11/2026 2:23:30 PM. This article is licensed under a Creative Commons Attribution-NonCommercial 3.0 Unported Licence.

by applying only one impedance test in different dimensions, like different temperatures and at different stages of life. Another article also applied EIS to measure the state of charge (SoC) and obtained a high accuracy model.[294] By using a sensitivity analysis of data, researchers extracted most reliable features to predict the SoC. These methods help improving the prediction of battery conditions, and also benefit sampling methods of EIS.

In conclusion, to make predictions for state of charge and health, researchers design a lot of machine learning algorithms and models, combining different characterization methods. These models provide valuable insights for designing and optimizing battery systems and accelerate the prediction, which are helpful for high throughput screening. Furthermore, by combining more physics insights with current machine learning algorithms, researchers can create models that can better explain the results.

6. Perspective

Despite numerous models that have been developed, machine learning-based energy chemistry is still in its early stages and there is still much room for improvement. In this section, we provide several perspectives based on our own knowledge and the relevant studies. We will focus more on the challenges and opportunities of machine learning in energy chemistry rather than the general problem of AI for science like data bias or limited data.

6.1 Concept transformation: from drugs to energy materials

Over the past 20 years, drug-based machine learning has made significant progress, and become an important field in cheminformatics. This machine learning expertise is now being applied to energy chemistry, specifically in the field of OPVs which draws on many concepts and techniques from drug-based machine learning. For example, molecular fingerprints, such as MACCS, and Morgan fingerprints, were initially proposed and developed in small molecule drug research for virtual screening and molecular similarity comparison, but it has recently been widely applied in the field of organic photovoltaics in energy chemistry. Besides, the concept of QSPR has been adapted from the drug discovery field to the field of OPVs and other material machine learning work. In the relatively early stages of machine learning in energy chemistry, it is worthwhile to consider the inspiration and guidance from drug design. This concept can help to speed up the development of machine learning in energy chemistry and lead to more effective and efficient solutions.

More recently, drug design for small molecules has kept pace with the development of applications in the field of SOTA machine learning technology, such as different transformer-based and GNN-based methods. But OPV machine learning models, which are also based on organic small molecule representation, are relatively limited and many of the current works still rely on using molecular fingerprinting with traditional machine learning. Compared to deep learning, traditional supervised learning requires less data and is more robust. This advantage can be extended and more adapted to the drawbacks of a small number of OPV datasets and low standardization of experimental data collected from the literature, which leads to better performance. However, using supervised learning cannot model complex relationships. With the development of OPVs and OPV data growth, the deep learning method could lead to a deeper understanding of underlying relationships in OPVs.

Transferring molecule-based models from one application to another is often simple since many molecule-based models have a high degree of applicability. For example, Some models based on small molecules can be used not only in drug discovery, but also in other areas such as materials science. Flam-Shepherd *et al.* showcased that their fragment-based 3D molecules model[295] can be used in the design of both drug molecules and the materials of organic light-emitting devices (OLED). Besides, with relatively minor modifications, some molecule-based generalizable models such as SMILES transformer reported by Shion Honda *et al.*[296] and SSVAE deep generative model reported by Kang *et al.*[297] could potentially be used in other molecule-based prediction models in energy chemistry.

6.2 Trustworthy models

The lack of interpretability and experimental validation can be a major limitation for many applications of chemical machine learning, especially in the discovery of energy relevant materials. Without understanding the underlying mechanisms of a model's predictions and whether those predictions are reliable, it can be difficult for researchers to trust and use the model effectively because a model's predictions may not always be accurate. Researchers can use different methods to make their works into white-box models, which provide insights into how models work internally. This allows researchers to have a better understanding of the mechanisms behind their predictions and decision-making processes.

Generally, some tools can help us to improve the interpretability of our models. Using visualization tools based on the NLP model or NN can visualize the weights of certain layers in a deep learning model. In some famous machine learning packages such as TensorFlow and Keras, it is easy to realize. This can make the model more acceptable; Rives *et al.* proposed a ESM-1b model which showed promising results in protein structural and functional prediction.[298] They used the tsne technique to visualize their trained weight in their ESM-1b model and illustrated that the ESM-1b model can learn the physical and chemical information from the protein sequence. Besides the visualization tool, one useful tool is model-agnostic methods[299] including the local interpretable model-agnostic explanations (LIME), SHAP, recursive feature elimination (RFE). The key attribute of model-agnostic methods is their independence from specific model structures, enabling their application across various model types. This flexibility allows for broad adoption in different model configurations.

© 2023 The Author(s). Published by the Royal Society of Chemistry

Open Access Article. Published on 24 April 2023. Downloaded on 2/11/2026 2:23:30 PM.
This article is licensed under a Creative Commons Attribution-NonCommercial 3.0 Unported Licence.

In addition, experimental validation is an important part of ensuring the overall acceptance of the work by the researchers. With the development of chemistry machine learning, different researchers will come up with different solutions for the same task. Machine learning models with experimental validation are more acceptable to the people who want to apply them.

6.3 Benchmark and criteria

There are different criteria reported in different papers for manually collecting and incorporating data in the field of machine learning in energy chemistry. It is extremely difficult to determine which method is best suited for a particular project, which highlights the importance of benchmarking and comparison studies. To objectively evaluate different types of models and descriptors, benchmark and the comparison criteria should be established in a same downstream task. Using the public benchmark and criteria, researchers can have a better understanding of the strengths and weaknesses of each method.

In many fields of machine learning, such as linguistics and biochemistry, many benchmarks have been established. Benchmark is one of the most important aspects of comparing models, which helps to clearly compare the performance of different models on different datasets. For molecules, several molecule benchmarks were set by Wu *et al.*[300] and Nigam *et al.*[78] However, more benchmarks are still needed to develop because many novel models in machine learning in chemistry are focusing on the descriptor and different works claim that their strategy is excellent but the training and test environments are different. Therefore, it is hard to compare different strategies. Although there are many public datasets for energy chemistry as mentioned above, we hope to have more public datasets in the future. Most of the current public datasets are collected in different methods, the average accuracy of validation with different datasets can be considered as an evaluation benchmark.

In summary, establishing more benchmarks helps to compare the quality of the corresponding algorithms or descriptors, which is more conducive to the development of chemical machine learning especially in energy chemistry.

6.4 Combining large language models with chemical science

The development of large language models (LLMs) has been very fast in recent years.[301] Although LLMs have shown promising results in predicting protein structures and generation in the field of protein modeling, the use of LLM models in the field of materials science is still in its early stages. There are several LLMs that have been developed for molecules, such as DPA-1 and Molformer, which can be applied to potential energy surfaces and encoding molecules.[302,303] In terms of extracting data from the materials science literature, there has been some recent progress. For example, MatBERT is a Bert-based model, which could be utilized to understand materials terminologies and paragraph-level scientific reasoning and achieve state-of-art results in several benchmark tests.[302,303] These models can be used in specific downstream tasks after fine-tuning. In the future, we believe that in specific areas, we will see more and more applications of LLMs.

Some LLMs, such as ChatGPT, are designed to help computers understand human language and generate natural language responses, making them valuable tools for various natural language processing (NLP) tasks. Such a chatbot could provide an accessible interaction way for researchers to leverage machine learning models, even if they are not familiar with programming or high-performance computing systems. Unluckily, a material-specific chatbot has not yet been developed. Nevertheless, the emergence of material-specific chatbots like ChatGPT that can interface with various downstream tasks and allow users to use pre-trained models for machine learning research is expected to lower the barrier to entry for machine learning research.

There is still much work to be done in this area. One challenge in building a LLM is the need for large amounts of high-quality data to train the model. Another challenge is to develop more specialized algorithms and architectures to handle the complex nature of materials science data. Despite these challenges, the development of LLMs has opened up new possibilities in the field of chemistry, and we can expect to see more exciting applications in the future.

Author contributions

Yuzhi Xu is responsible for conceptualization, finding resources, investigation, writing original drafts, and reviews and editing. Jiankai Ge is responsible for conceptualization, finding resources, investigation, writing original drafts, reviews and editing, and project administration. Cheng-Wei Ju is responsible for conceptualization, investigation, reviews and editing, and project administration.

Conflicts of interest

There are no conflicts to declare.

Acknowledgements

We would like to express our gratitude to those who supported us in the revision of this review. Thanks to Zhewei Li from Tsinghua University for helping with proofreading. We also appreciate the invitation from The Royal Society of Chemistry.

Notes and references

1 K. Li and B. Lin, *Renewable Sustainable Energy Rev.*, 2015, **52**, 1107–1122.
2 G. R. Monama, K. E. Ramohlola, E. I. Iwuoha and K. D. Modibane, *Results Chem.*, 2022, 100321.
3 A. Pudi, A. P. Karcz, S. Keshavarz, V. Shadravan, M. P. Andersson and S. S. Mansouri, *Chem. Eng. Process.*, 2022, **174**, 108883.
4 A. Goeppert, M. Czaun, J.-P. Jones, G. S. Prakash and G. A. Olah, *Chem. Soc. Rev.*, 2014, **43**, 7995–8048.

Open Access Article. Published on 24 April 2023. Downloaded on 2/11/2026 2:23:30 PM. This article is licensed under a Creative Commons Attribution-NonCommercial 3.0 Unported Licence.

5 D.-D. Zhou, X.-W. Zhang, Z.-W. Mo, Y.-Z. Xu, X.-Y. Tian, Y. Li, X.-M. Chen and J.-P. Zhang, *EnergyChem*, 2019, **1**, 100016.
6 I. Dincer and C. Acar, *Inter. J. Energy Res.*, 2015, **39**, 585–606.
7 K. T. Butler, D. W. Davies, H. Cartwright, O. Isayev and A. Walsh, *Nature*, 2018, **559**, 547–555.
8 A. C. Mater and M. L. Coote, *J. Chem. Inf. Model.*, 2019, **59**, 2545–2559.
9 M. Meuwly, *Chem. Rev.*, 2021, **121**, 10218–10239.
10 P. K. Nayak, S. Mahesh, H. J. Snaith and D. Cahen, *Nat. Rev. Mater.*, 2019, **4**, 269–285.
11 T. G. Allen, J. Bullock, X. Yang, A. Javey and S. De Wolf, *Nat. Energy*, 2019, **4**, 914–928.
12 A. Polman, M. Knight, E. C. Garnett, B. Ehrler and W. C. Sinke, *Science*, 2016, **352**, aad4424.
13 G. C. Righini and F. Enrichi, *Sol. Cells Light Manage.*, 2020, 1–32.
14 J. Zhang, W. Zhang, H.-M. Cheng and S. R. P. Silva, *Mater. Today*, 2020, **39**, 66–88.
15 Z. Wan, Q.-D. Wang, D. Liu and J. Liang, *Comput. Mater. Sci.*, 2021, **198**, 110699.
16 A. Jain, Y. Shin and K. A. Persson, *Nat. Rev. Mater.*, 2016, **1**, 1–13.
17 X. Zhou, J. Jankowska, H. Dong and O. V. Prezhdo, *J. Energy Chem.*, 2018, **27**, 637–649.
18 Y. S. Meng and M. E. Arroyo-de Dompablo, *Energy Environ. Sci.*, 2009, **2**, 589–609.
19 L. Wang, G. Nan, X. Yang, Q. Peng, Q. Li and Z. Shuai, *Chem. Soc. Rev.*, 2010, **39**, 423–434.
20 R. Ramprasad, R. Batra, G. Pilania, A. Mannodi-Kanakkithodi and C. Kim, *npj Comput. Mater.*, 2017, **3**, 54.
21 B. Ryu, L. Wang, H. Pu, M. K. Chan and J. Chen, *Chem. Soc. Rev.*, 2022, **51**, 1899–1925.
22 N.-T. Suen, S.-F. Hung, Q. Quan, N. Zhang, Y.-J. Xu and H. M. Chen, *Chem. Soc. Rev.*, 2017, **46**, 337–365.
23 N. Dubouis and A. Grimaud, *Chem. Sci.*, 2019, **10**, 9165–9181.
24 C. Kim, F. Dionigi, V. Beermann, X. Wang, T. Möller and P. Strasser, *Adv. Mater.*, 2019, **31**, 1805617.
25 F. M. Sapountzi, J. M. Gracia, H. O. Fredriksson and J. H. Niemantsverdriet, *et al.*, *Prog. Energy Combust. Sci.*, 2017, **58**, 1–35.
26 Z. Liang, H. Zheng and R. Cao, *ChemElectroChem*, 2019, **6**, 2600–2614.
27 C. Wei, S. Sun, D. Mandler, X. Wang, S. Z. Qiao and Z. J. Xu, *Chem. Soc. Rev.*, 2019, **48**, 2518–2534.
28 A. Chen, X. Zhang and Z. Zhou, *InfoMat*, 2020, **2**, 553–576.
29 X. Zhang, Y. Tian, L. Chen, X. Hu and Z. Zhou, *J. Phys. Chem. Lett.*, 2022, **13**, 7920–7930.
30 Z. Zhou, *J. Mater. Chem. A*, 2021, **9**, 1295–1296.
31 Z.-H. Zhou, *Machine learning*, Springer Nature, 2021.
32 S. Palkovits, *ChemCatChem*, 2020, **12**, 3995–4008.
33 A. Bender, N. Schneider, M. Segler, W. Patrick Walters, O. Engkvist and T. Rodrigues, *Nat. Rev. Chem.*, 2022, **6**, 428–442.
34 D. Zou, D. Wang, Z. Chu, Z. Lv and X. Fan, *Coord. Chem. Rev.*, 2010, **254**, 1169–1178.
35 C. J. Emmott, J. A. Röhr, M. Campoy-Quiles, T. Kirchartz, A. Urbina, N. J. Ekins-Daukes and J. Nelson, *Energy Environ. Sci.*, 2015, **8**, 1317–1328.
36 Y. Hu, J. Wang, C. Yan and P. Cheng, *Nat. Rev. Mater.*, 2022, 1–3.
37 A. Mahmood and J.-L. Wang, *Energy Environ. Sci.*, 2021, **14**, 90–105.
38 P. C. St. John, C. Phillips, T. W. Kemper, A. N. Wilson, Y. Guan, M. F. Crowley, M. R. Nimlos and R. E. Larsen, *J. Chem. Phys.*, 2019, **150**, 234111.
39 J. Hachmann, R. Olivares-Amaya, S. Atahan-Evrenk, C. Amador-Bedolla, R. S. Sánchez-Carrera, A. Gold-Parker, L. Vogt, A. M. Brockway and A. Aspuru-Guzik, *J. Phys. Chem. Lett.*, 2011, **2**, 2241–2251.
40 S. A. Lopez, E. O. Pyzer-Knapp, G. N. Simm, T. Lutzow, K. Li, L. R. Seress, J. Hachmann and A. Aspuru-Guzik, *Sci. Data*, 2016, **3**, 1–7.
41 T. W. David, H. Anizelli, P. Tyagi, C. Gray, W. Teahan and J. Kettle, *IEEE J. Photovolt.*, 2019, **9**, 1768–1773.
42 H. Sahu, F. Yang, X. Ye, J. Ma, W. Fang and H. Ma, *J. Mater. Chem. A*, 2019, **7**, 17480–17488.
43 K. Wu, B. Natarajan, L. Morkowchuk, M. Krein and C. M. Breneman, *Inf. Mater. Sci. Eng.*, Elsevier, 2013, pp. 385–422.
44 Y. Miyake and A. Saeki, *J. Phys. Chem. Lett.*, 2021, **12**, 12391–12401.
45 Z.-W. Zhao, M. del Cueto, Y. Geng and A. Troisi, *Chem. Mater.*, 2020, **32**, 7777–7787.
46 K. Kranthiraja and A. Saeki, *Adv. Funct. Mater.*, 2021, **31**, 2011168.
47 D. Weininger, *J. Chem. Inf. Comput. Sci.*, 1988, **28**, 31–36.
48 U. V. Ucak, I. Ashyrmamatov and J. Lee, Chemrxiv, 2022.
49 N. O'Boyle and A. Dalke, Chemrxiv, 2018.
50 M. Krenn, F. Häse, A. Nigam, P. Friederich and A. Aspuru-Guzik, *Machine Learning: Sci. Tech.*, 2020, **1**, 045024.
51 Y. Xu, C.-W. Ju, B. Li, Q.-S. Ma, Z. Chen, L. Zhang and J. Chen, *ACS Appl. Mater. Interfaces*, 2021, **13**, 34033–34042.
52 L. Himanen, M. O. Jäger, E. V. Morooka, F. F. Canova, Y. S. Ranawat, D. Z. Gao, P. Rinke and A. S. Foster, *Comput. Phys. Commun.*, 2020, **247**, 106949.
53 H. Sahu, W. Rao, A. Troisi and H. Ma, *Adv. Energy Mater.*, 2018, **8**, 1801032.
54 A. Cereto-Massagué, M. J. Ojeda, C. Valls, M. Mulero, S. Garcia-Vallvé and G. Pujadas, *Methods*, 2015, **71**, 58–63.
55 H. Kubinyi, *Encycl. Comput. Chem.*, 1998, **1**, 448–460.
56 D. C. Elton, Z. Boukouvalas, M. D. Fuge and P. W. Chung, *Mol. Syst. Design Engineering*, 2019, **4**, 828–849.
57 S. Riniker and G. A. Landrum, *J. Cheminformatics*, 2013, **5**, 1–17.
58 P. Xu, H. Chen, M. Li and W. Lu, *Adv. Theory Simul.*, 2022, **5**, 2100565.
59 Q. Zhang, Y. J. Zheng, W. Sun, Z. Ou, O. Odunmbaku, M. Li, S. Chen, Y. Zhou, J. Li and B. Qin, *et al.*, *Adv. Sci.*, 2022, **9**, 2104742.

© 2023 The Author(s). Published by the Royal Society of Chemistry

Open Access Article. Published on 24 April 2023. Downloaded on 2/11/2026 2:23:30 PM. This article is licensed under a Creative Commons Attribution-NonCommercial 3.0 Unported Licence.

60 W. Sun, Y. Zheng, K. Yang, Q. Zhang, A. A. Shah, Z. Wu, Y. Sun, L. Feng, D. Chen and Z. Xiao, *et al.*, *Sci. Adv.*, 2019, **5**, eaay4275.
61 H. Matter and T. Pötter, *J. Chem. Inf. Comput. Sci.*, 1999, **39**, 1211–1225.
62 Y. Wu, J. Guo, R. Sun and J. Min, *npj Comput. Mater.*, 2020, **6**, 1–8.
63 S. Nagasawa, E. Al-Naamani and A. Saeki, *J. Phys. Chem. Lett.*, 2018, **9**, 2639–2646.
64 Z. Xiong, D. Wang, X. Liu, F. Zhong, X. Wan, X. Li, Z. Li, X. Luo, K. Chen and H. Jiang, *et al.*, *J. Medic. Chem.*, 2019, **63**, 8749–8760.
65 A. Eibeck, D. Nurkowski, A. Menon, J. Bai, J. Wu, L. Zhou, S. Mosbach, J. Akroyd and M. Kraft, *ACS Omega*, 2021, **6**, 23764–23775.
66 P. Han, P. Zhao, C. Lu, J. Huang, J. Wu, S. Shang, B. Yao and X. Zhang, Proceedings of the AAAI Conference on Artificial Intelligence, 2022, pp. 4014–4021.
67 H. Wang, W. Li, X. Jin, K. Cho, H. Ji, J. Han and M. D. Burke, *arXiv* Preprint arXiv:2109.09888, 2021.
68 D. Padula, J. D. Simpson and A. Troisi, *Mater. Horizons*, 2019, **6**, 343–349.
69 M.-H. Lee, *Adv. Intell. Syst.*, 2020, **2**, 1900108.
70 T. W. David, H. Anizelli, T. J. Jacobsson, C. Gray, W. Teahan and J. Kettle, *Nano Energy*, 2020, **78**, 105342.
71 A. Nigam, R. Pollice, M. Krenn, G. dos Passos Gomes and A. Aspuru-Guzik, *Chem. Sci.*, 2021, **12**, 7079–7090.
72 C. Kunkel, J. T. Margraf, K. Chen, H. Oberhofer and K. Reuter, *Nat. Commun.*, 2021, **12**, 1–11.
73 Z. Chen, J. Li and Y. Xu, *arXiv*, 2021, Preprint arXiv:2107.02613.
74 A. Saeki and K. Kranthiraja, *Jpn. J. Appl. Phys.*, 2019, **59**, SD0801.
75 M. Lee and K. Min, *J. Chem. Inf. Model.*, 2022, **62**(12), 2943–2950.
76 Y. Xu, K. Lin, S. Wang, L. Wang, C. Cai, C. Song, L. Lai and J. Pei, *Future Med. Chem.*, 2019, **11**, 567–597.
77 T. Sousa, J. Correia, V. Pereira and M. Rocha, *J. Chem. Inf. Model.*, 2021, **61**, 5343–5361.
78 A. Nigam, R. Pollice, G. Tom, K. Jorner, L. A. Thiede, A. Kundaje and A. Aspuru-Guzik, *arXiv*, 2022, Preprint arXiv:2209.12487.
79 X. Du, L. Lüer, T. Heumueller, J. Wagner, C. Berger, T. Osterrieder, J. Wortmann, S. Langner, U. Vongsaysy and M. Bertrand, *et al.*, *Joule*, 2021, **5**, 495–506.
80 S. Langner, F. Häse, J. D. Perea, T. Stubhan, J. Hauch, L. M. Roch, T. Heumueller, A. Aspuru-Guzik and C. J. Brabec, *Adv. Mater.*, 2020, **32**, 1907801.
81 T. Wolfram and S. Ellialtioglu, *Electronic and optical properties of d-band perovskites*, Cambridge University Press, Cambridge, 2006.
82 H. S. Jung and N.-G. Park, *Small*, 2015, **11**, 10–25.
83 J. Tian, Q. Xue, Q. Yao, N. Li, C. J. Brabec and H.-L. Yip, *Adv. Energy Mater.*, 2020, **10**, 2000183.
84 N. S. Kumar and K. C. B. Naidu, *J. Materiomics*, 2021, **7**, 940–956.
85 Q. Xu, D. Yang, J. Lv, Y.-Y. Sun and L. Zhang, *Small Methods*, 2018, **2**, 1700316.
86 C. Zhang, C. Liu, Y. Gao, S. Zhu, F. Chen, B. Huang, Y. Xie, Y. Liu, M. Ma and Z. Wang, *et al.*, *Adv. Sci.*, 2022, 2204138.
87 A. Fakharuddin, M. K. Gangishetty, M. Abdi-Jalebi, S.-H. Chin, A. bin Mohd Yusoff, D. N. Congreve, W. Tress, F. Deschler, M. Vasilopoulou and H. J. Bolink, *et al.*, *Nat. Electron.*, 2022, **5**, 203–216.
88 C. Zhao, D. Zhang and C. Qin, *CCS Chem.*, 2020, **2**, 859–869.
89 Z. Bian, Z. Wang, B. Jiang, P. Hongmanorom, W. Zhong and S. Kawi, *Renewable Sustainable Energy Rev.*, 2020, **134**, 110291.
90 J. Hwang, R. R. Rao, L. Giordano, Y. Katayama, Y. Yu and Y. Shao-Horn, *Science*, 2017, **358**, 751–756.
91 J. Yu, R. Ran, Y. Zhong, W. Zhou, M. Ni and Z. Shao, *Energy Environ. Mater.*, 2020, **3**, 121–145.
92 S. Narayanan, N. Parikh, M. M. Tavakoli, M. Pandey, M. Kumar, A. Kalam, S. Trivedi, D. Prochowicz and P. Yadav, *Eur. J. Inorg. Chem.*, 2021, 1201–1212.
93 Y. Rong, Y. Hu, A. Mei, H. Tan, M. I. Saidaminov, S. I. Seok, M. D. McGehee, E. H. Sargent and H. Han, *Science*, 2018, **361**, eaat8235.
94 Y. Zhang, Y. Ma, Y. Wang, X. Zhang, C. Zuo, L. Shen and L. Ding, *Adv. Mater.*, 2021, **33**, 2006691.
95 M. R. Filip and F. Giustino, *Proc. Natl. Acad. Sci. U. S. A.*, 2018, **115**, 5397–5402.
96 S. C. Tidrow, *Ferroelectrics*, 2014, **470**, 13–27.
97 D. Ji, S. Feng, L. Wang, S. Wang, M. Na, H. Zhang, C. Zhang and X. Li, *Vacuum*, 2019, **164**, 186–193.
98 C. J. Bartel, C. Sutton, B. R. Goldsmith, R. Ouyang, C. B. Musgrave, L. M. Ghiringhelli and M. Scheffler, *Sci. Adv.*, 2019, **5**, eaav0693.
99 S. Lu, Q. Zhou, L. Ma, Y. Guo and J. Wang, *Small Methods*, 2019, **3**, 1900360.
100 D. Jain, S. Chaube, P. Khullar, S. G. Srinivasan and B. Rai, *Phys. Chem. Chem. Phys.*, 2019, **21**, 19423–19436.
101 G. Pilania, P. V. Balachandran, C. Kim and T. Lookman, *Front. Mater.*, 2016, **3**, 19.
102 C. Li, H. Hao, B. Xu, Z. Shen, E. Zhou, D. Jiang and H. Liu, *Comput. Mater. Sci.*, 2021, **198**, 110714.
103 R. Ouyang, S. Curtarolo, E. Ahmetcik, M. Scheffler and L. M. Ghiringhelli, *Phys. Rev. Mater.*, 2018, **2**, 083802.
104 R. Ouyang, E. Ahmetcik, C. Carbogno, M. Scheffler and L. M. Ghiringhelli, *J. Phys.: Mater.*, 2019, **2**, 024002.
105 J. L. Teunissen and F. Da Pieve, *J. Phys. Chem. C*, 2021, **125**, 25316–25326.
106 S. R. Xie, P. Kotlarz, R. G. Hennig and J. C. Nino, *Comput. Mater. Sci.*, 2020, **180**, 109690.
107 P. Xu, D. Chang, T. Lu, L. Li, M. Li and W. Lu, *J. Chem. Inf. Model.*, 2022, **62**(21), 5038–5049.
108 Z. Wan, Q.-D. Wang and J. Liang, *Int. J. Quantum Chem.*, 2021, **121**, e26441.
109 Z. Wan, Q.-D. Wang, D. Liu and J. Liang, *New J. Chem.*, 2021, **45**, 9427–9433.
110 C. Chen, W. Ye, Y. Zuo, C. Zheng and S. P. Ong, *Chem. Mater.*, 2019, **31**, 3564–3572.

Open Access Article. Published on 24 April 2023. Downloaded on 2/11/2026 2:23:30 PM. This article is licensed under a Creative Commons Attribution-NonCommercial 3.0 Unported Licence.

111 G. H. Gu, J. Jang, J. Noh, A. Walsh and Y. Jung, *npj Comput. Mater.*, 2022, **8**, 1–8.
112 P. Omprakash, B. Manikandan, A. Sandeep, R. Shrivastava, P. Viswesh and D. B. Panemangalore, *Comput. Mater. Sci.*, 2021, **196**, 110530.
113 Q. Zhou, P. Tang, S. Liu, J. Pan, Q. Yan and S.-C. Zhang, *Proc. Natl. Acad. Sci. U. S. A.*, 2018, **115**, E6411–E6417.
114 A. Ihalage and Y. Hao, *npj Comput. Mater.*, 2021, **7**, 1–12.
115 Y. Dan, Y. Zhao, X. Li, S. Li, M. Hu and J. Hu, *npj Comput. Mater.*, 2020, **6**, 1–7.
116 L. Wei, Q. Li, Y. Song, S. Stefanov, E. Siriwardane, F. Chen and J. Hu, *arXiv*, 2022, Preprint arXiv:2204.11953.
117 C. W. Myung, A. Hajibabaei, J.-H. Cha, M. Ha, J. Kim and K. S. Kim, *Adv. Energy Mater.*, 2022, 2202279.
118 L. Zhang, M. He and S. Shao, *Nano Energy*, 2020, **78**, 105380.
119 Z. Guo and B. Lin, *Sol. Energy*, 2021, **228**, 689–699.
120 L. Xu, L. Wencong, P. Chunrong, S. Qiang and G. Jin, *Comput. Mater. Sci.*, 2009, **46**, 860–868.
121 G.-Q. Liang and J. Zhang, *Comput. Mater. Sci.*, 2022, **204**, 111172.
122 W. Li, R. Jacobs and D. Morgan, *Comput. Mater. Sci.*, 2018, **150**, 454–463.
123 C. Kim, G. Pilania and R. Ramprasad, *J. Phys. Chem. C*, 2016, **120**, 14575–14580.
124 J. Li, Y. Peng, L. Zhao, G. Chen, L. Zeng, G. Wei and Y. Xu, *Mater. Adv.*, 2022, **3**, 8639–8646.
125 L. Williams, A. Mukherjee and K. Rajan, *J. Phys. Chem. Lett.*, 2020, **11**, 7462–7468.
126 E. I. Marchenko, S. A. Fateev, A. A. Petrov, V. V. Korolev, A. Mitrofanov, A. V. Petrov, E. A. Goodilin and A. B. Tarasov, *Chem. Mater.*, 2020, **32**, 7383–7388.
127 Y. Zhang and X. Xu, *CrystEngComm*, 2020, **22**, 6385–6397.
128 Y. Zhang and X. Xu, *ChemistrySelect*, 2020, **5**, 9999–10009.
129 R. Li, Q. Deng, D. Tian, D. Zhu and B. Lin, *Crystals*, 2021, **11**, 818.
130 W. A. Saidi, W. Shadid and I. E. Castelli, *npj Comput. Mater.*, 2020, **6**, 1–7.
131 P. V. Balachandran, A. A. Emery, J. E. Gubernatis, T. Lookman, C. Wolverton and A. Zunger, *Phys. Rev. Mater.*, 2018, **2**, 043802.
132 V. Shetty, S. Shedthi and J. Kumaraswamy, *Mater. Today: Proc.*, 2022, **52**, 457–461.
133 J. Kim, E. Kim and K. Min, *Adv. Theory and Simul.*, 2021, **4**, 2100263.
134 W. Zheng, H. Cheng, Y. Liu, L. Chen, Y. Guo, Y. Yang, X. Yan and D. Wu, *Comput. Mater. Sci.*, 2022, **209**, 111394.
135 I. M. Pendleton, M. K. Caucci, M. Tynes, A. Dharna, M. A. N. Nellikkal, Z. Li, E. M. Chan, A. J. Norquist and J. Schrier, *J. Phys. Chem. C*, 2020, **124**, 13982–13992.
136 L. Li, Q. Tao, P. Xu, X. Yang, W. Lu and M. Li, *Comput. Mater. Sci.*, 2021, **199**, 110712.
137 A. Talapatra, B. P. Uberuaga, C. R. Stanek and G. Pilania, *Chem. Mater.*, 2021, **33**, 845–858.
138 H. A. Jame, S. Sarker, M. S. Islam, M. T. Islam, A. Rauf, S. Ahsan, S. S. Nishat, M. R. Jani, K. M. Shorowordi and J. Carbonara, *et al.*, *ACS Appl. Mater. Interfaces*, 2021, **14**, 502–516.
139 F. Massuyeau, T. Broux, F. Coulet, A. Demessence, A. Mesbah and R. Gautier, *Adv. Mater.*, 2022, 2203879.
140 J. Yang and A. Mannodi-Kanakkithodi, *MRS Bull.*, 2022, 1–9.
141 J. C. Stanley, F. Mayr and A. Gagliardi, *Adv. Theory Simul.*, 2020, **3**, 1900178.
142 S. Lu, Q. Zhou, Y. Ouyang, Y. Guo, Q. Li and J. Wang, *Nat. Commun.*, 2018, **9**, 1–8.
143 Z. Gao, H. Zhang, G. Mao, J. Ren, Z. Chen, C. Wu, I. D. Gates, W. Yang, X. Ding and J. Yao, *Appl. Surface Sci.*, 2021, **568**, 150916.
144 Y. Wu, S. Lu, M.-G. Ju, Q. Zhou and J. Wang, *Nanoscale*, 2021, **13**, 12250–12259.
145 W. Hu, L. Zhang and Z. Pan, *ACS Appl. Mater. Interfaces*, 2022, **14**(18), 21596–21604.
146 E. Meyer, D. Mutukwa, N. Zingwe and R. Taziwa, *Metals*, 2018, **8**, 667.
147 Ç. Odabas and R. Yldrm, *Energy Tech.*, 2020, **8**, 1901449.
148 R. Jaafreh, A. Sharan, M. Sajjad, N. Singh and K. Hamad, *Adv. Funct. Mater.*, 2022, 2210374.
149 J. M. Howard, E. M. Tennyson, B. R. Neves and M. S. Leite, *Joule*, 2019, **3**, 325–337.
150 F. Häse, L. M. Roch, P. Friederich and A. Aspuru-Guzik, *Nat. Commun.*, 2020, **11**, 1–11.
151 M. C. Swain and J. M. Cole, *J. Chem. Inf. Model.*, 2016, **56**, 1894–1904.
152 D. M. Jessop, S. E. Adams, E. L. Willighagen, L. Hawizy and P. Murray-Rust, *J. Cheminformatics*, 2011, **3**, 1–12.
153 L. Hawizy, D. M. Jessop, N. Adams and P. Murray-Rust, *J. Cheminformatics*, 2011, **3**, 1–13.
154 M. Krallinger, O. Rabal, A. Lourenco, J. Oyarzabal and A. Valencia, *Chem. Rev.*, 2017, **117**, 7673–7761.
155 H. Huo, Z. Rong, O. Kononova, W. Sun, T. Botari, T. He, V. Tshitoyan and G. Ceder, *npj Comput. Mater.*, 2019, **5**, 1–7.
156 O. Kononova, T. He, H. Huo, A. Trewartha, E. A. Olivetti and G. Ceder, *Iscience*, 2021, **24**, 102155.
157 E. J. Beard and J. M. Cole, *Sci. Data*, 2022, **9**, 1–19.
158 E. Kim, Z. Jensen, A. van Grootel, K. Huang, M. Staib, S. Mysore, H.-S. Chang, E. Strubell, A. McCallum and S. Jegelka, *et al.*, *J. Chem. Inf. Model.*, 2020, **60**, 1194–1201.
159 J. Wei, X. Chu, X.-Y. Sun, K. Xu, H.-X. Deng, J. Chen, Z. Wei and M. Lei, *InfoMat*, 2019, **1**, 338–358.
160 W. Yan, Y. Liu, Y. Zang, J. Cheng, Y. Wang, L. Chu, X. Tan, L. Liu, P. Zhou and W. Li, *et al.*, *Nano Energy*, 2022, 107394.
161 S. Sun, N. T. Hartono, Z. D. Ren, F. Oviedo, A. M. Buscemi, M. Layurova, D. X. Chen, T. Ogunfunmi, J. Thapa and S. Ramasamy, *et al.*, *Joule*, 2019, **3**, 1437–1451.
162 J. Kirman, A. Johnston, D. A. Kuntz, M. Askerka, Y. Gao, P. Todorović, D. Ma, G. G. Privé and E. H. Sargent, *Matter*, 2020, **2**, 938–947.
163 Ç. Odabas and R. Yldrm, *Sol. Energy Mater. Sol. Cells*, 2020, **205**, 110284.
164 Y. Yu, X. Tan, S. Ning and Y. Wu, *ACS Energy Lett.*, 2019, **4**, 397–404.

© 2023 The Author(s). Published by the Royal Society of Chemistry

Open Access Article. Published on 24 April 2023. Downloaded on 2/11/2026 2:23:30 PM. This article is licensed under a Creative Commons Attribution-NonCommercial 3.0 Unported Licence.

165 N. T. P. Hartono, J. Thapa, A. Tiihonen, F. Oviedo, C. Batali, J. J. Yoo, Z. Liu, R. Li, D. F. Marrón and M. G. Bawendi, *et al.*, *Nat. Commun.*, 2020, **11**, 1–9.
166 A. Senocrate, T. Acartürk, G. Y. Kim, R. Merkle, U. Starke, M. Grätzel and J. Maier, *J. Mater. Chem. A*, 2018, **6**, 10847–10855.
167 S. Jariwala, S. Burke, S. Dunfield, R. C. Shallcross, M. Taddei, J. Wang, G. E. Eperon, N. R. Armstrong, J. J. Berry and D. S. Ginger, *Chem. Mater.*, 2021, **33**, 5035–5044.
168 X. Cai, F. Liu, A. Yu, J. Qin, M. Hatamvand, I. Ahmed, J. Luo, Y. Zhang, H. Zhang and Y. Zhan, *Light: Sci. Appl.*, 2022, **11**, 1–12.
169 Y. Hu, X. Hu, L. Zhang, T. Zheng, J. You, B. Jia, Y. Ma, X. Du, L. Zhang and J. Wang, *et al.*, *Adv. Energy Mater.*, 2022, 2201463.
170 R. W. Epps, K. C. Felton, C. W. Coley and M. Abolhasani, *Lab Chip*, 2017, **17**, 4040–4047.
171 M. Seifrid, R. Pollice, A. Aguilar-Granda, Z. Morgan Chan, K. Hotta, C. T. Ser, J. Vestfrid, T. C. Wu and A. Aspuru-Guzik, *Acc. Chem. Research*, 2022, **55**, 2454–2466.
172 M. Ahmadi, M. Ziatdinov, Y. Zhou, E. A. Lass and S. V. Kalinin, *Joule*, 2021, **5**, 2797–2822.
173 Z. Li, M. A. Najeeb, L. Alves, A. Z. Sherman, V. Shekar, P. Cruz Parrilla, I. M. Pendleton, W. Wang, P. W. Nega and M. Zeller, *et al.*, *Chem. Mater.*, 2020, **32**, 5650–5663.
174 S. Greenhill, S. Rana, S. Gupta, P. Vellanki and S. Venkatesh, *IEEE Access*, 2020, **8**, 13937–13948.
175 Q. Song, Y. Bai and Q. Chen, *J. Phys. Chem. Lett.*, 2022, **13**, 10741–10750.
176 B. P. MacLeod, F. G. Parlane, T. D. Morrissey, F. Häse, L. M. Roch, K. E. Dettelbach, R. Moreira, L. P. Yunker, M. B. Rooney and J. R. Deeth, *et al.*, *Sci. Adv.*, 2020, **6**, eaaz8867.
177 L. M. Roch, F. Häse, C. Kreisbeck, T. Tamayo-Mendoza, L. P. Yunker, J. E. Hein and A. Aspuru-Guzik, *Sci. Robotics*, 2018, **3**, eaat5559.
178 K. Higgins, S. M. Valleti, M. Ziatdinov, S. V. Kalinin and M. Ahmadi, *ACS Energy Lett.*, 2020, **5**, 3426–3436.
179 Z.-Y. Zhou, N. Tian, J.-T. Li, I. Broadwell and S.-G. Sun, *Chem. Soc. Rev.*, 2011, **40**, 4167–4185.
180 S. P. Fisher, A. W. Tomich, S. Lovera, J. F. Kleinsasser, J. Guo, M. Asay, H. Nelson and V. Lavallo, *Chem. Rev.*, 2019, **119**, 8262–8290.
181 M. Stamatakis and D. G. Vlachos, *ACS Catal.*, 2012, **2**, 2648–2663.
182 M. P. Duduković, F. Larachi and P. L. Mills, *Catal. Rev.*, 2002, **44**, 123–246.
183 J. Huang, F. Cheng, B. P. Binks and H. Yang, *J. Am. Chem. Soc.*, 2015, **137**, 15015–15025.
184 E. L. Clark, J. Wong, A. J. Garza, Z. Lin, M. Head-Gordon and A. T. Bell, *J. Am. Chem. Soc.*, 2019, **141**, 4191–4193.
185 J. Greeley, J. K. Nørskov and M. Mavrikakis, *Annu. Rev. Phys. Chem.*, 2002, **53**, 319–348.
186 A. Nilsson, L. Pettersson, B. Hammer, T. Bligaard, C. H. Christensen and J. K. Nørskov, *Catal. Lett.*, 2005, **100**, 111–114.
187 J. Ge and B. Peters, *Chem. Eng. J.*, 2023, **466**, 143251.
188 B. Smit, *J. Chem. Phys.*, 1992, **96**, 8639–8640.
189 A. C. Van Duin, S. Dasgupta, F. Lorant and W. A. Goddard, *J. Phys. Chem. A*, 2001, **105**, 9396–9409.
190 S. J. Marrink, H. J. Risselada, S. Yefimov, D. P. Tieleman and A. H. De Vries, *J. Phys. Chem. B*, 2007, **111**, 7812–7824.
191 J. N. Canongia Lopes and A. A. Pádua, *Theor. Chem. Acc.*, 2012, **131**, 1–11.
192 E. Vignola, S. N. Steinmann, B. D. Vandegehuchte, D. Curulla, M. Stamatakis and P. Sautet, *J. Chem. Phys.*, 2017, **147**, 054106.
193 J. Westermayr, M. Gastegger, M. F. Menger, S. Mai, L. González and P. Marquetand, *Chem. Sci.*, 2019, **10**, 8100–8107.
194 J. Behler and M. Parrinello, *Phys. Rev. Lett.*, 2007, **98**, 146401.
195 J. Behler, *J. Chem. Phys.*, 2011, **134**, 074106.
196 A. P. Bartók, M. C. Payne, R. Kondor and G. Csányi, *Phys. Rev. Lett.*, 2010, **104**, 136403.
197 A. P. Bartók, R. Kondor and G. Csányi, *Phys. Rev. B: Condens. Matter Mater. Phys.*, 2013, **87**, 184115.
198 A. P. Thompson, L. P. Swiler, C. R. Trott, S. M. Foiles and G. J. Tucker, *J. Comp. Phys.*, 2015, **285**, 316–330.
199 K. T. Schütt, H. E. Sauceda, P.-J. Kindermans, A. Tkatchenko and K.-R. Müller, *J. Chem. Phys.*, 2018, **148**, 241722.
200 J. Gasteiger, J. Groß and S. Günnemann, *Proc. Int. Conf. Learn. Represent.*, 2019.
201 H. Wang, L. Zhang, J. Han and E. Weinan, *Comput. Phys. Commun.*, 2018, **228**, 178–184.
202 S.-D. Huang, C. Shang, P.-L. Kang, X.-J. Zhang and Z.-P. Liu, *Wiley Interdiscip. Rev.: Comput. Mol. Sci.*, 2019, **9**, e1415.
203 A. Khorshidi and A. A. Peterson, *Comput. Phys. Commun.*, 2016, **207**, 310–324.
204 K. Schutt, P. Kessel, M. Gastegger, K. Nicoli, A. Tkatchenko and K.-R. Muller, *J. Chem. Theory Comput.*, 2018, **15**, 448–455.
205 K. T. Schutt, S. S. Hessmann, N. W. Gebauer, J. Lederer and M. Gastegger, arXiv, 2022, preprint arXiv:2212.05517.
206 A. Shapeev, *Multiscale Model. Simul.*, 2016, **14**, 1153–1173.
207 E. V. Podryabinkin and A. V. Shapeev, *Comput. Mater. Sci.*, 2017, **140**, 171–180.
208 K. Gubaev, E. V. Podryabinkin, G. L. W. Hart and A. V. Shapeev, *Comput. Mater. Sci.*, 2019, **156**, 148–156.
209 B. Hammer and J. K. Norskov, *Nature*, 1995, **376**, 238–240.
210 I. Takigawa, K.-i Shimizu, K. Tsuda and S. Takakusagi, *RSC Adv.*, 2016, **6**, 52587–52595.
211 Z. Lian, M. Yang, F. Jan and B. Li, *J. Phys. Chem. Lett.*, 2021, **12**, 7053–7059.
212 T. Xie and J. C. Grossman, *Phys. Rev. Lett.*, 2018, **120**, 145301.
213 R. Bashyam and P. Zelenay, *Nature*, 2006, **443**, 63–66.
214 T. Zhou, H. Shan, H. Yu, C. Zhong, J. Ge, N. Zhang, W. Chu, W. Yan, Q. Xu and H. Wu, *et al.*, *Adv. Mater.*, 2020, **32**, 2003251.

Open Access Article. Published on 24 April 2023. Downloaded on 2/11/2026 2:23:30 PM. This article is licensed under a Creative Commons Attribution-NonCommercial 3.0 Unported Licence.

215 X. Yu, T. Zhou, J. Ge and C. Wu, *ACS Mater. Lett.*, 2020, **2**, 1423–1434.
216 C. Zhong, T. Zhou, N. Zhang, M. Chen, Y. Xie, W. Yan, W. Chu, X. Zheng, Q. Xu, J. Ge and C. Wu, 2023, **53**(3), 0304.
217 P. Chen, T. Zhou, L. Xing, K. Xu, Y. Tong, H. Xie, L. Zhang, W. Yan, W. Chu and C. Wu, *et al.*, *Angew. Chem., Int. Ed.*, 2017, **129**, 625–629.
218 J. Zhang, Y. Zhao, C. Chen, Y.-C. Huang, C.-L. Dong, C.-J. Chen, R.-S. Liu, C. Wang, K. Yan and Y. Li, *et al.*, *J. Am. Chem. Soc.*, 2019, **141**, 20118–20126.
219 Z. Jin, P. Li, Y. Meng, Z. Fang, D. Xiao and G. Yu, *Nat. Catal.*, 2021, **4**, 615–622.
220 Y. Ying, K. Fan, X. Luo, J. Qiao and H. Huang, *J. Mater. Chem. A*, 2021, **9**, 16860–16867.
221 W. Ye, S. Chen, Y. Lin, L. Yang, S. Chen, X. Zheng, Z. Qi, C. Wang, R. Long and M. Chen, *et al.*, *Chem*, 2019, **5**, 2865–2878.
222 N. Zhang, T. Zhou, J. Ge, Y. Lin, Z. Du, W. Wang, Q. Jiao, R. Yuan, Y. Tian and W. Chu, *et al.*, *Matter*, 2020, **3**, 509–521.
223 H. Surden, *Wash. L. Rev.*, 2014, **89**, 87.
224 T. Toyao, Z. Maeno, S. Takakusagi, T. Kamachi, I. Takigawa and K.-I. Shimizu, *ACS Catal.*, 2019, **10**, 2260–2297.
225 P. Schlexer Lamoureux, K. T. Winther, J. A. Garrido Torres, V. Streibel, M. Zhao, M. Bajdich, F. Abild-Pedersen and T. Bligaard, *ChemCatChem*, 2019, **11**, 3581–3601.
226 X. Zhu, J. Yan, M. Gu, T. Liu, Y. Dai, Y. Gu and Y. Li, *J. Phys. Chem. Lett.*, 2019, **10**, 7760–7766.
227 J. H. Friedman, *Comput. Stat. Data Anal.*, 2002, **38**, 367–378.
228 V. Viswanathan, A. H. Epstein, Y.-M. Chiang, E. Takeuchi, M. Bradley, J. Langford and M. Winter, *Nature*, 2022, **601**, 519–525.
229 X. Ke, Y. Liang, L. Ou, H. Liu, Y. Chen, W. Wu, Y. Cheng, Z. Guo, Y. Lai and P. Liu, *et al.*, *Energy Storage Mater.*, 2019, **23**, 547–555.
230 Y. Chen, X. Ke, Y. Cheng, M. Fan, W. Wu, X. Huang, Y. Liang, Y. Zhong, Z. Ao and Y. Lai, *et al.*, *Energy Storage Mater.*, 2020, **26**, 56–64.
231 J. Xiao, Q. Li, Y. Bi, M. Cai, B. Dunn, T. Glossmann, J. Liu, T. Osaka, R. Sugiura and B. Wu, *et al.*, *Nat. Energy*, 2020, **5**, 561–568.
232 Y. Zhu, X. He and Y. Mo, *J. Mater. Chem. A*, 2016, **4**, 3253–3266.
233 C. Wang, A. Wang, L. Ren, X. Guan, D. Wang, A. Dong, C. Zhang, G. Li and J. Luo, *Adv. Funct. Mater.*, 2019, **29**, 1905940.
234 Y. Liang, Y. Chen, X. Ke, Z. Zhang, W. Wu, G. Lin, Z. Zhou and Z. Shi, *J. Mater. Chem. A*, 2020, **8**, 18094–18105.
235 G. Liu, Y. Yang, X. Lu, F. Qi, Y. Liang, A. Trukhanov, Y. Wu, Z. Sun and X. Lu, *ACS Appl. Mater. Interfaces*, 2022, **14**, 31803–31813.
236 D. Liu, W. Zhu, J. Trottier, C. Gagnon, F. Barray, A. Guerfi, A. Mauger, H. Groult, C. Julien and J. Goodenough, *et al.*, *RSC Adv.*, 2014, **4**, 154–167.
237 S. B. Peterson, J. Apt and J. Whitacre, *J. Power Sources*, 2010, **195**, 2385–2392.
238 P. K. Nayak, E. M. Erickson, F. Schipper, T. R. Penki, N. Munichandraiah, P. Adelhelm, H. Sclar, F. Amalraj, B. Markovsky and D. Aurbach, *Adv. Energy Mater.*, 2018, **8**, 1702397.
239 Y. Xie, M. Naguib, V. N. Mochalin, M. W. Barsoum, Y. Gogotsi, X. Yu, K.-W. Nam, X.-Q. Yang, A. I. Kolesnikov and P. R. Kent, *J. Am. Chem. Soc.*, 2014, **136**, 6385–6394.
240 G. Liu, N. Wang, F. Qi, X. Lu, Y. Liang and Z. Sun, *Inorg. Chem. Front.*, 2023, **10**, 699–711.
241 L. Yaohua, K. Xi, L. Jun and S. Zhicong, *Energy Storage Sci. Tech.*, 2017, **6**, 1.
242 X. Ke, Z. Zhang, Y. Cheng, Y. Liang, Z. Tan, J. Liu, L. Liu, Z. Shi and Z. Guo, *Sci. China Mater.*, 2018, **61**, 353–362.
243 R. P. Joshi, J. Eickholt, L. Li, M. Fornari, V. Barone and J. E. Peralta, *ACS Appl. Mater. Interfaces*, 2019, **11**, 18494–18503.
244 S. P. Ong, W. D. Richards, A. Jain, G. Hautier, M. Kocher, S. Cholia, D. Gunter, V. L. Chevrier, K. A. Persson and G. Ceder, *Comput. Mater. Sci.*, 2013, **68**, 314–319.
245 A. Jain, S. P. Ong, G. Hautier, W. Chen, W. D. Richards, S. Dacek, S. Cholia, D. Gunter, D. Skinner and G. Ceder, *et al.*, *APL Mater.*, 2013, **1**, 011002.
246 S. P. Ong, V. L. Chevrier, G. Hautier, A. Jain, C. Moore, S. Kim, X. Ma and G. Ceder, *Energy Environ. Sci.*, 2011, **4**, 3680–3688.
247 J. C. Bachman, S. Muy, A. Grimaud, H.-H. Chang, N. Pour, S. F. Lux, O. Paschos, F. Maglia, S. Lupart and P. Lamp, *et al.*, *Chem. Rev.*, 2016, **116**, 140–162.
248 Z. Zhang, Y. Shao, B. Lotsch, Y.-S. Hu, H. Li, J. Janek, L. F. Nazar, C.-W. Nan, J. Maier and M. Armand, *et al.*, *Energy Environ. Sci.*, 2018, **11**, 1945–1976.
249 A. D. Sendek, E. D. Cubuk, E. R. Antoniuk, G. Cheon, Y. Cui and E. J. Reed, *Chem. Mater.*, 2018, **31**, 342–352.
250 Y. Zhang, X. He, Z. Chen, Q. Bai, A. M. Nolan, C. A. Roberts, D. Banerjee, T. Matsunaga, Y. Mo and C. Ling, *Nat. Commun.*, 2019, **10**, 1–7.
251 H. Xu, J. Zhu, D. P. Finegan, H. Zhao, X. Lu, W. Li, N. Hoffman, A. Bertei, P. Shearing and M. Z. Bazant, *Adv. Energy Mater.*, 2021, **11**, 2003908.
252 A. N. Mistry, K. Smith and P. P. Mukherjee, *ACS Appl. Mater. Interfaces*, 2018, **10**, 6317–6326.
253 S. Hein, J. Feinauer, D. Westhoff, I. Manke, V. Schmidt and A. Latz, *J. Power Sources*, 2016, **336**, 161–171.
254 S. J. An, J. Li, C. Daniel, D. Mohanty, S. Nagpure and D. L. Wood III, *Carbon*, 2016, **105**, 52–76.
255 E. Peled and S. Menkin, *J. Electrochem. Soc.*, 2017, **164**, A1703.
256 H. Zhang, C. Li, M. Piszcz, E. Coya, T. Rojo, L. M. Rodriguez-Martinez, M. Armand and Z. Zhou, *Chem. Soc. Rev.*, 2017, **46**, 797–815.
257 Z. Wang, Y. Sun, L. Chen and X. Huang, *J. Electrochem. Soc.*, 2004, **151**, A914.
258 L. O. Valøen and J. N. Reimers, *J. Electrochem. Soc.*, 2005, **152**, A882.
259 S. Lux, I. Lucas, E. Pollak, S. Passerini, M. Winter and R. Kostecki, *Electrochem. Commun.*, 2012, **14**, 47–50.

© 2023 The Author(s). Published by the Royal Society of Chemistry

Open Access Article. Published on 24 April 2023. Downloaded on 2/11/2026 2:23:30 PM.
This article is licensed under a Creative Commons Attribution-NonCommercial 3.0 Unported Licence.

260 R. Jalem, M. Nakayama and T. Kasuga, *J. Mater. Chem. A*, 2014, **2**, 720–734.
261 N. Kireeva and V. S. Pervov, *Phys. Chem. Chem. Phys.*, 2017, **19**, 20904–20918.
262 S.-H. Kim, K.-H. Choi, S.-J. Cho, E.-H. Kil and S.-Y. Lee, *J. Mater. Chem. A*, 2013, **1**, 4949–4955.
263 X.-B. Cheng, T.-Z. Hou, R. Zhang, H.-J. Peng, C.-Z. Zhao, J.-Q. Huang and Q. Zhang, *Adv. Mater.*, 2016, **28**, 2888–2895.
264 Z. Ahmad, T. Xie, C. Maheshwari, J. C. Grossman and V. Viswanathan, *ACS Cent. Sci.*, 2018, **4**, 996–1006.
265 Y.-T. Chen, M. Duquesnoy, D. H. Tan, J.-M. Doux, H. Yang, G. Deysher, P. Ridley, A. A. Franco, Y. S. Meng and Z. Chen, *ACS Energy Lett.*, 2021, **6**, 1639–1648.
266 D. P. Tabor, L. M. Roch, S. K. Saikin, C. Kreisbeck, D. Sheberla, J. H. Montoya, S. Dwaraknath, M. Aykol, C. Ortiz and H. Tribukait, *et al.*, *Nat. Rev. Mater.*, 2018, **3**, 5–20.
267 K. A. Severson, P. M. Attia, N. Jin, N. Perkins, B. Jiang, Z. Yang, M. H. Chen, M. Aykol, P. K. Herring and D. Fraggedakis, *et al.*, *Nat. Energy*, 2019, **4**, 383–391.
268 K. Goebel, B. Saha, A. Saxena, J. R. Celaya and J. P. Christophersen, *IEEE Instrum. Meas. Mag.*, 2008, **11**, 33–40.
269 M.-F. Ng, J. Zhao, Q. Yan, G. J. Conduit and Z. W. Seh, *Nat. Mach. Intell.*, 2020, **2**, 161–170.
270 A. E. Ruehli, *IEEE Trans. Microw. Theory Tech.*, 1974, **22**, 216–221.
271 X. Hu, S. Li and H. Peng, *J. Power Sources*, 2012, **198**, 359–367.
272 D. P. Finegan, J. Zhu, X. Feng, M. Keyser, M. Ulmefors, W. Li, M. Z. Bazant and S. J. Cooper, *Joule*, 2021, **5**, 316–329.
273 V. R. Subramanian, V. Boovaragavan and V. D. Diwakar, *Electrochem. Solid-State Lett.*, 2007, **10**, A255.
274 V. Boovaragavan, S. Harinipriya and V. R. Subramanian, *J. Power Sources*, 2008, **183**, 361–365.
275 S. S. Mansouri, P. Karvelis, G. Georgoulas and G. Nikolakopoulos, *IFAC-PapersOnLine*, 2017, **50**, 4727–4732.
276 G. O. Sahinoglu, M. Pajovic, Z. Sahinoglu, Y. Wang, P. V. Orlik and T. Wada, *IEEE Trans. Ind. Electron.*, 2017, **65**, 4311–4321.
277 P. Khumprom and N. Yodo, *Energies*, 2019, **12**, 660.
278 P. M. Attia, A. Grover, N. Jin, K. A. Severson, T. M. Markov, Y.-H. Liao, M. H. Chen, B. Cheong, N. Perkins and Z. Yang, *et al.*, *Nature*, 2020, **578**, 397–402.
279 H. Zou and T. Hastie, *J. R. Stat. Soc. Series B Stat. Methodol.*, 2005, **67**, 301–320.
280 M. Hoffman, B. Shahriari and N. Freitas, *Artificial Intelligence and Statistics*, 2014, pp. 365–374.
281 A. Grover, T. Markov, P. Attia, N. Jin, N. Perkins, B. Cheong, M. Chen, Z. Yang, S. Harris and W. Chueh, *et al.*, International Conference on Artificial Intelligence and Statistics, 2018, pp. 833–842.
282 Z. Tong, J. Miao, S. Tong and Y. Lu, *J. Clean. Prod.*, 2021, **317**, 128265.
283 C. K. Chan, X. F. Zhang and Y. Cui, *Nano Lett.*, 2008, **8**, 307–309.
284 M. Saubanère, E. McCalla, J.-M. Tarascon and M.-L. Doublet, *Energy Environ. Sci.*, 2016, **9**, 984–991.
285 M. Freire, N. V. Kosova, C. Jordy, D. Chateigner, O. Lebedev, A. Maignan and V. Pralong, *Nat. Mater.*, 2016, **15**, 173–177.
286 S. Abu-Sharkh and D. Doerffel, *J. Power Sources*, 2004, **130**, 266–274.
287 A. Maheshwari, N. G. Paterakis, M. Santarelli and M. Gibescu, *Appl. Energy*, 2020, **261**, 114360.
288 A. A. Franco, *RSC Adv.*, 2013, **3**, 13027–13058.
289 D. D. Macdonald, *Electrochim. Acta*, 2006, **51**, 1376–1388.
290 P. Singh, R. Vinjamuri, X. Wang and D. Reisner, *Electrochim. Acta*, 2006, **51**, 1673–1679.
291 C. T. Love, M. B. Virji, R. E. Rocheleau and K. E. Swider-Lyons, *J. Power Sources*, 2014, **266**, 512–519.
292 N. S. Spinner, C. T. Love, S. L. Rose-Pehrsson and S. G. Tuttle, *Electrochim. Acta*, 2015, **174**, 488–493.
293 Y. Zhang, Q. Tang, Y. Zhang, J. Wang, U. Stimming and A. A. Lee, *Nat. Commun.*, 2020, **11**, 1–6.
294 I. Babaeiyazdi, A. Rezaei-Zare and S. Shokrzadeh, *Energy*, 2021, **223**, 120116.
295 D. Flam-Shepherd, A. Zhigalin and A. Aspuru-Guzik, arXiv, 2022, preprint arXiv:2202.00658.
296 S. Honda, S. Shi and H. R. Ueda, arXiv, 2019, preprint arXiv:1911.04738.
297 S. Kang and K. Cho, *J. Chem. Inf. Model.*, 2018, **59**, 43–52.
298 A. Rives, J. Meier, T. Sercu, S. Goyal, Z. Lin, J. Liu, D. Guo, M. Ott, C. L. Zitnick and J. Ma, *et al.*, *Proc. Natl. Acad. Sci. U. S. A.*, 2021, **118**, e2016239118.
299 R. Dybowski, *New J. Chem.*, 2020, **44**, 20914–20920.
300 Z. Wu, B. Ramsundar, E. N. Feinberg, J. Gomes, C. Geniesse, A. S. Pappu, K. Leswing and V. Pande, *Chem. Sci.*, 2018, **9**, 513–530.
301 Y. Hu and M. J. Buehler, *APL Machine Learning*, 2023, **1**, 010901.
302 D. Zhang, H. Bi, F.-Z. Dai, W. Jiang, L. Zhang and H. Wang, arXiv, 2022, preprint arXiv:2208.08236.
303 A. Trewartha, N. Walker, H. Huo, S. Lee, K. Cruse, J. Dagdelen, A. Dunn, K. A. Persson, G. Ceder and A. Jain, *Patterns*, 2022, **3**, 100488.